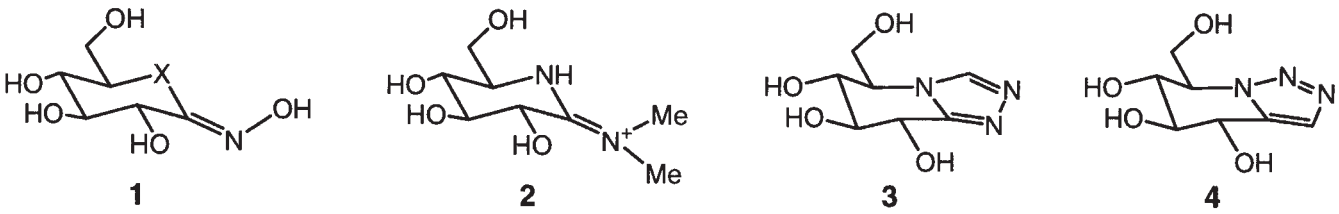

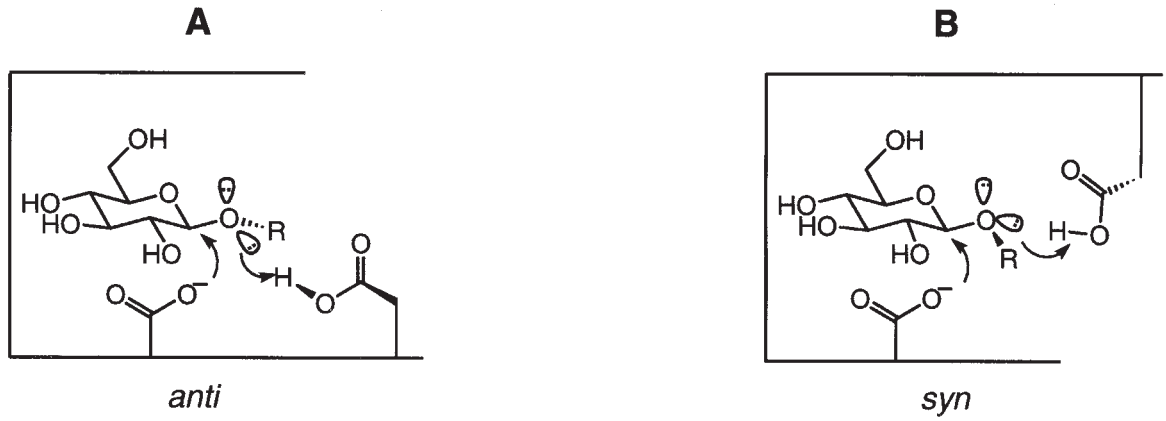

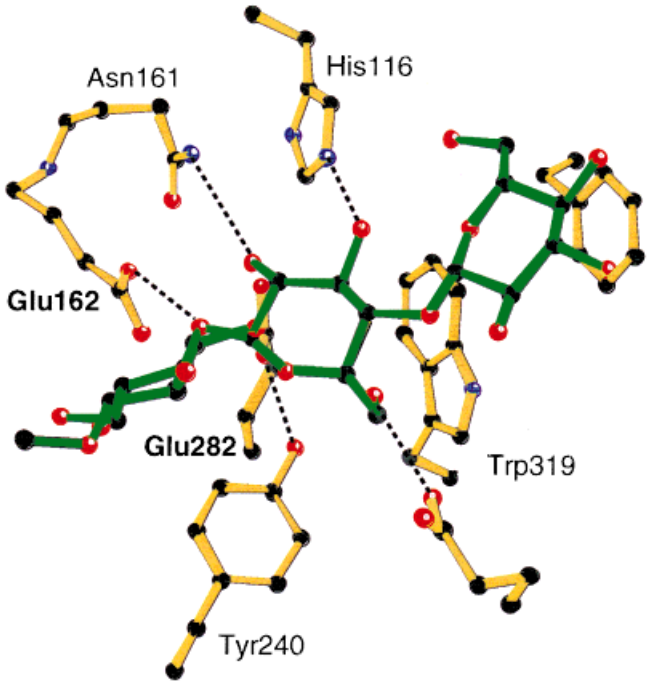

Complex of the endocellulase from *Acidothermus cellulolyticus* with cellotetraose

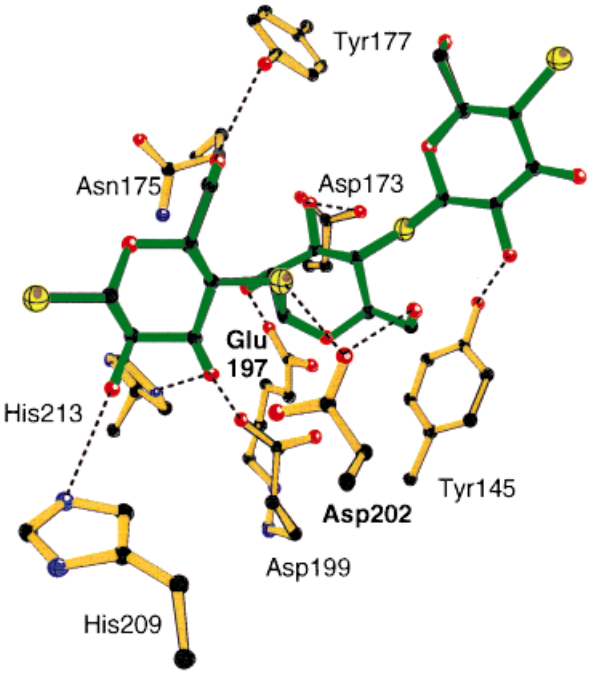

Complex of the cellobiohydrolase from *Fusarium oxysporum* with a thioglycoside

Insights into the detailed mechanism of action of glycosidases have been gained by combining the study of the kinetics of inhibitors such as **1**–**4** with the analysis of crystal structures of glycosidases and glycosidase–ligand complexes. Configuration-retaining *β*-glycosidases do not protonate their substrate "from above", but "from the side", either *anti* (**A**) or *syn* to the endocyclic C1–O bond (**B**).

Recent Insights into Inhibition, Structure, and Mechanism of Configuration-Retaining Glycosidases

Tom D. Heightman and Andrea T. Vasella*

Dedicated to Professor Duilio Arigoni on the occasion of his 70th birthday

Until recently, the design of highly potent, selective glycosidase inhibitors has been patterned upon the analogy with the structure of natural products with established activity as glycosidase inhibitors or with the structure of the hypothetical reactive intermediate closest to the transition state, that is, an oxycarbenium cation. Relationships between the structure of the inhibitors and the kinetic data have rarely been examined in a systematic way, and there are no standards universally adopted for the chromogenic substrate, the pH value, the buffer, and the enzymes analyzed. However, the systematic variation of key structural parameters of inhibitors, combined with the interpretation of standardized kinetic data, is a powerful method for the analysis of the enzymic mechanism. The combination of these data with the information available from the growing number of crystal structure analyses of glycosidases, in some cases in complexes with ligands, provides the opportunity to correlate the inhibition with the structure of both the inhibitor and the enzyme. In view of the relationship between the structures of glycosidases for which X-ray data are available, and the structures of glycosidases of the same family of which only the amino acid sequence is known, such correlations acquire an exemplary and thus particularly valuable character; they can be readily tested as the number of protein X-ray analyses increases. This information provides a detailed rational basis for the design of selective and potent inhibitors and for the interpretation of subtle differences of reaction mechanism. This is itself of interest, even disregarding the potential applications of strong and selective inhibitors as antiviral, antidiabetic, and antifungal agents. Our review describes recent progress in the design, synthesis, and characterization of inhibitors of O-pyranosidases in light of the increasing availability of enzymic structural information.

Keywords: azoles · enzyme inhibitors · glycosidases · lactams · protonations

1. Introduction

Glycosidases and their inhibitors have enjoyed much research interest in the last decade, much of which has been reviewed.[1–22] The application of naturally occurring glycosidases in enzyme replacement therapy; in textile, food, and pulp processing; and as catalysts in oligosaccharide synthesis has encouraged the engineering of proteins with improved catalytic properties and stability. Inhibitors of glycosidases, already used or tested in the treatment of diabetes and HIV infection and as antifungal agents, are expected to arouse increasing interest as therapeutic agents as our understanding of the role of glycosidases in recognition processes improves.

[*] Prof. Dr. A. T. Vasella, Dr. T. D. Heightman
Laboratorium für Organische Chemie
ETH-Zentrum
Universitätstrasse 16, CH-8092 Zürich (Switzerland)
Fax: (+41) 1-632-11-36
E-mail: vasella@sugar.org.chem.ethz.ch

The enzymic cleavage of the glycosidic bond liberates a sugar hemiacetal with either the same configuration as the substrate (retention) or, less commonly, the opposite configuration (inversion). The catalytic mechanism for configuration-retaining glycosidases proposed by Koshland in 1953 has, despite refinement in many details, stood the test of time.[23] In the currently accepted form of this mechanism (Figure 1a), the aglycon is activated as a leaving group by coordination of the exocyclic oxygen atom with an enzymic acidic function (catalytic acid HA; partial protonation by a carboxyl group).[24, 25] More or less concerted attack of a carboxylate group (catalytic nucleophile B^-) located on the opposite side of the plane of the pyranose ring leads to a glycosyl ester intermediate.[26, 27] The degree of concertedness of bond breaking and bond making is unclear, although both extremes (S_N2 or S_N1) are unlikely.[28] The aglycon diffuses away from the active site and is replaced with a water molecule; the reverse process takes place: this water molecule is partially deprotonated by the conjugate base of the catalytic acid, attacks the anomeric carbon, and cleaves the newly formed

  1433-7851/99/3806-0751 $ 17.50+.50/0

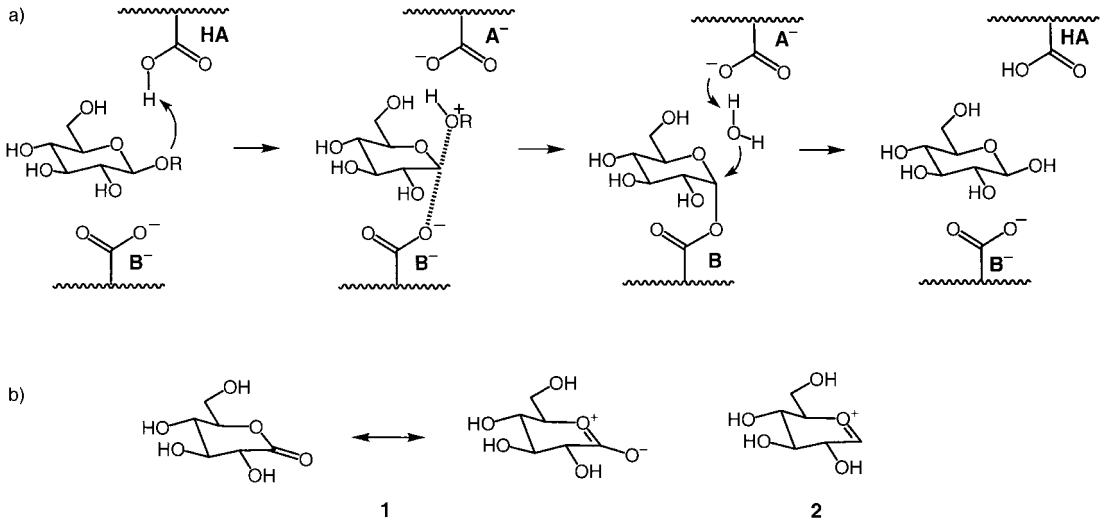

Figure 1. a) Catalytic mechanism for configuration-retaining glycosidases according to Koshland.[23] b) Glucono-1,5-lactone **1** as a transition state analogue.

glycosyl ester bond. The double inversion leads to overall retention of configuration. This review will highlight the essential data and interpretations that have changed our understanding of aspects of the mechanism of configuration-retaining glycosidases in recent years.

Table 1. K_i values [μM] of the lactone **1** and the piperidines **3**, **4**, and **5**.

Enzyme (source)	**1**	**3**[29]	**4**[30, 31]	**5**[32]
α-glucosidase (brewers' yeast)	2000	330	14.6	> 1500
β-glucosidase (almonds)	400	2.8	18	1.5
β-glucosidase (*Agrobacterium faecalis*)	1.4	–	–	–

2. Lactones and Piperidines: Neutral and Basic Inhibitors

2.1. Shape or Charge?

The observation that glyconolactones such as **1** (Figure 1 b, Table 1) are relatively strong inhibitors of β-glycosidases was first made in 1940 by Ezaki[33] and confirmed by Horikoshi in 1942, who studied the β-glucosidases from *Aspergillus* and from almonds.[34] Levvy and Conchie later made the same observation with other glycosidases.[35–37] Leaback pointed to the "stereochemical and conformational similarities between the lactone and the transition state in the enzyme-catalyzed pyranoside hydrolysis",[38] and Reese et al.[39] added that the polar oxy group also partially mimics the positive charge of the oxycarbenium ion intermediate **2** (Figure 1 b). The relative importance of these two features, shape and charge,[40] has remained the subject of much debate, much more so than their correlation with details of the enzymic mechanism.[41–45] Pauling had emphasized the importance of "shape" when he expounded that an enzyme should bind the transition state more strongly than the substrate in order to effectively catalyze a reaction, and thus transition state analogues should be potent inhibitors.[41] The transition state for glycoside hydrolysis must have some considerable resemblance to the hypothetical oxycarbenium ion intermediate, leading

Andrea T. Vasella studied chemistry and biology in Fribourg (Switzerland). In 1971 he obtained his Ph.D. in the group of Duilio Arigoni at the ETH Zürich, then worked in the research groups of Jack Baldwin and R. B. Woodward, and returned in 1974 to the ETH Zürich. He became Assistant Professor in Fribourg, moved to the Universität Zürich in 1981, and joined the ETH Zürich in 1993, where he continues his research on carbohydrates.

Tom D. Heightman, born in 1971 in Chelmsford (UK), received his MA in chemistry at the University of Oxford in 1993. After moving to the ETH Zürich, he obtained his doctorate in 1998 in the research group of Professor Vasella with a thesis on the design, synthesis, and evaluation of glycosidase inhibitors and DNA ligands. He is now investigator at SmithKline Beecham Pharmaceuticals in Harlow.

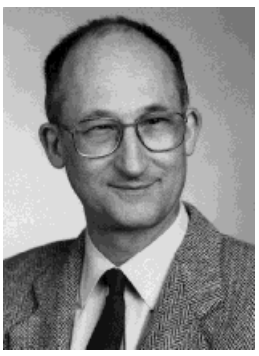

A. T. Vasella

T. D. Heightman

Leaback and Reese to suggest that the lactones are analogues of the reactive intermediate and, hence, of the transition state.

The importance of charge was emphasized by the modeling of substrates and inhibitors in the active site of lysozyme based on X-ray structure analysis, suggesting that a carboxylate group was implicated in stabilizing the oxycarbenium ion intermediate without the formation of a glycosyl ester.[46] It was generally agreed that the analogous interaction of the catalytic carboxylate group with the dipole of the lactone contributed to its strong inhibition of lysozyme.[47–50]

The catalytic carboxyl and carboxylate groups were later shown—by a combination of irreversible inhibitor labeling, site-directed mutagenesis, and sequence alignments—to be almost ubiquitous in glycosidases.[51, 52] The protonated form of naturally occurring basic inhibitors, including nojirimycin (**3**), deoxynojirimycin (**4**), and castanospermine (**5**), must be bound by charge–charge interactions.[53] Certainly, with their

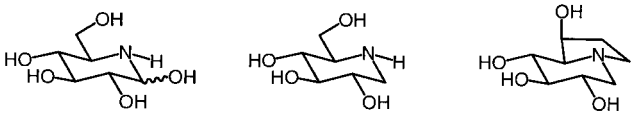

3 **4** **5**

sp^3-hybridized anomeric carbon atom and chair conformation they resemble the shape of the oxycarbenium ion less than the lactone. Interaction with the catalytic carboxyl/carboxylate groups thus provided a rational basis for the design of new inhibitors, although it was not clear whether the interaction was with the catalytic nucleophile or the carboxylate derived from deprotonation of the catalytic acid by the basic inhibitor.[30, 54]

Many researchers have asked the questions: why is the neutral lactone **1** as good a β-glycosidase inhibitor as the positively charged piperidines **3**–**5**, and why, in contrast, is the lactone so much weaker in its inhibition of α-glycosidases, whereas the piperidines are stronger (Table 1)? Which factors are more important for inhibition of a given type of glycosidase: charge or the shape dictated by hybridization and the conformation of the pyranose or piperidinose ring? Are lactones and piperidines (and other basic inhibitors) really transition state analogues? Only if this is so will their study contribute in a rational way to a deeper understanding of the mechanism of action of glycosidases. The following describes, from the perspective of the reviewers, recent synthetic, kinetic, and structural research attempting to answer these and other questions.

2.2. Synthesis and Evaluation of Lactone Analogues

A disadvantage of the glycono-1,5-lactones is their tendency to undergo hydrolytic ring opening under mildly basic conditions and conversion into (inactive) 1,4-lactones under mildly acidic conditions, complicating the measurement of inhibition constants,[39, 55] and reducing the chances of obtaining crystalline enzyme–inhibitor complexes for X-ray analysis.[56] This may account for the fact that the transition state character of lactones has remained speculative. For these reasons, we turned to the study and design of lactone analogues. A first lactone analogue synthesized and studied by our group is the hydroximolactone **7**, prepared by oxidation of the hydroxy oximes **6**, which are in equilibrium with the corresponding cyclic hydroxylamines.[57] Like the lactone, **7** has a flattened chair conformation, but is stable to basic and

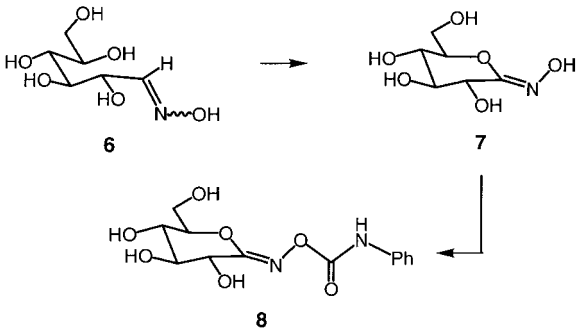

6 **7** **8**

mildly acidic hydrolysis and ring conversion. The additional hydroxyl group allows the introduction of substituents, potentially mimicking the aglycon. The unsubstituted hydroximolactone inhibits the sweet-almond β-glucosidases ten times more weakly than the lactone **1** (Table 2), but the phenylurethane **8** proved stronger, as would be anticipated

Table 2. K_i values [μM] at pH 6.8 of the lactone oximes **7** and **8**, the amidine **11**, the amidrazone **12**, and the lactam oxime **13** and at pH 4.5 of the lactone oximes **7** and **8**.

Enzyme (source)	**7**	**8**	**11**[58]	**12**[58]	**13**[58]
α-glucosidase (brewers' yeast)	6800	–	–	–	2.9
β-glucosidase (almonds) at pH 6.8	4300	43	10	8.4	14
β-glucosidase (almonds) at pH 4.5	98	2.3	–	–	–
β-glucosidase (*Agrobacterium faecalis*)	30	1.4	–	–	0.6
β-galactosidase (bovine liver)	–	–	–	19	–
α-mannosidase (jack beans)	–	–	9.0	3.1	–

from the preference of the almond enzymes for aromatic glycosides.[59] The transition state analogue character, however, remained speculative.

The next types of lactone analogues were designed to combine the sp^2-hybridized anomeric center of the lactone with the positive charge of the piperidines. The Ganem group synthesized the glyconoamidine **11** and the analogous lactam hydrazone **12** and hydroximolactam **13** by oxidation of the naturally occurring nojirimycin and activation of the resulting lactam **9** as the thionolactam **10**, allowing the introduction of nitrogen nucleophiles.[44, 58, 60]

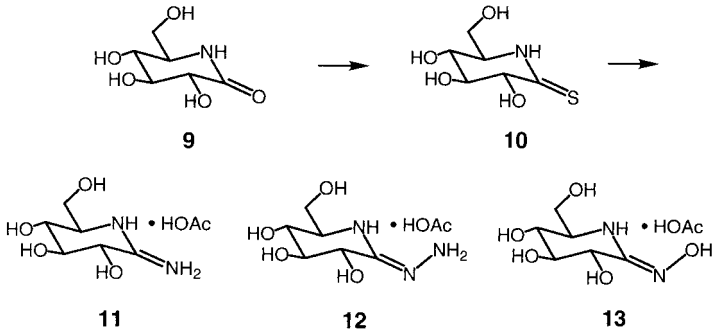

9 **10**

11 **12** **13**

All three lactone analogues **11**–**13** proved micromolar inhibitors of several α- and β-glycosidases (Table 2), leading Ganem et al. to call them "broad spectrum transition state analogues".[44] The latter contention was based on their proposal that these lactone analogues should be isomers of **11**–**13** with an endocyclic double bond, possess a half-chair conformation, and thus resemble the oxycarbenium ion intermediate (and thereby the transition state) more closely than the lactone **1** or the hydroximolactone **7**. The inhibition by the permanently protonated amidine **11** and lactam hydrazone **12** was shown to be pH independent, whilst that of the less basic hydroximolactam **13** was pH dependent, becoming weaker at pH values above 6. The inhibition results were interpreted in a fruitfully challenging way. The configuration was considered relatively unimportant. In spite of the high K_i value of **13** at pH 7, it was also concluded that, since the K_i values of **11**-**13** are similar (at pH 5) despite large differences in their pK_a values, "Mimicking the incipient charge buildup proved less important for enzyme inhibition than a flattened chair conformation, since even the relatively neutral amidoxime effectively blocked glycoside hydrolysis".[58] By interpolation (similar inhibition by the amidinium salt and the neutral **13**) this would mean that proton transfer to the inhibitor cannot be important.

We were challenged by the contention that these inhibitors are "broad spectrum transition state analogues": firstly because many glycosidases are configurationally selective, and their discrimination should be most pronounced in the transition state; and secondly because Ganem et al. considered enzymic protonation of the inhibitor as a relatively unimportant factor, whilst the substrate must be at least partially protonated by the enzyme in the transition state. Clearly the structure, pK value, and inhibitory activity of the hydroximolactam **13**—and the choice of the glycosidases[61]—were crucial to this interpretation. We therefore sought a practical synthesis of **13** and its two monolabeled ^{15}N isotopomers to verify its structure. The benzylated D-gluconolactam **17** (Bn = benzyl) was prepared in an overall yield of 70% from the corresponding lactone **14** by ammonolysis to the hydroxyamide **15** followed by an oxidoreduction.[62] Conversion of **17** into the hydroximolactam **13** was then

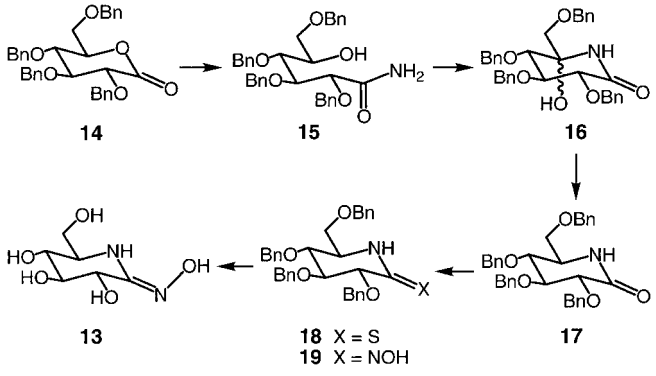

carried out via the thionolactam **18**.[63] ^1H and ^{15}N NMR spectroscopy and X-ray structure analysis of **13** clearly demonstrated that the double bond is exocyclic, and the ring a flattened chair (Figure 2). Upon protonation, **13** undergoes

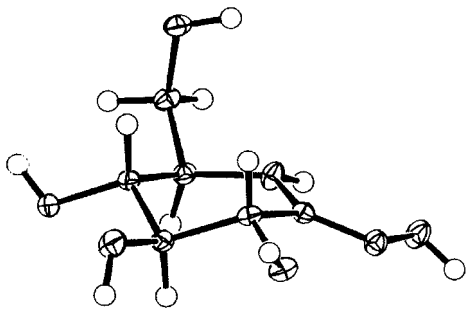

Figure 2. X-ray structure of **13**.

a conformational change to a half-chair, suggesting that protonation by the glycosidase is an important factor in the binding of **13**. The weaker inhibition of the hydroximolactone **7** as compared with that of the hydroximolactam **13** would then reflect its lower basicity. In keeping with this hypothesis, **7** proved a stronger inhibitor at pH 4.5 than at pH 6.8 (Table 2).

The binding of the basic derivatives **11** and **12**, which are protonated at pH values at least up to 7, is most probably driven by electrostatic interactions, as with the piperidines, and likewise results in poor configurational selectivity. The low pH dependency indicates that the main electrostatic interaction is with the catalytic nucleophile, which remains deprotonated throughout the pH range studied. The lack of configurational selectivity indicates that these inhibitors are at best partial transition state analogues. In addition, the selectivity of the inhibitor must be compared to the selectivity of the enzyme. It is known that the β-glucosidases from sweet almonds and the β-galactosidases from bovine liver, both used by Ganem et al., hydrolyze *gluco*-, and *galacto*-configured substrates about equally well.[64, 65] For the almond glycosidase the ratio of $V_{max}K_M^{-1}$ (glucoside) to $V_{max}K_M^{-1}$ (mannoside) is greater than 300,[30] whilst the inhibition by the *manno*-amidrazone and *manno*-hydroximolactam is only 24 and 15 times weaker, respectively, than that by the corresponding *gluco* analogues, which also renders an analogy between these inhibitors and the transition state unlikely.

2.3. Tetrazoles: Configurationally Selective Transition State Analogues

These results led us to ask the questions: are neutral, lactone-type inhibitors configurationally selective, and are they indeed transition state analogues? What is the effect of the ring conformation (chair versus half-chair) on the inhibitory potency and selectivity?

We designed the tetrazole **20** as a neutral, stable lactone analogue, the six-membered ring of which presumably having a half-chair conformation as a result of its fusion with the aromatic ring. The key step in the first synthesis of the tetrazole was the intramolecular 1,3-dipolar cycloaddition of a protected 5-azido-gluconononitrile.[66] This was prepared by transforming tetrabenzyl glucose into the open-chain gluconononitrile, inverting the configuration at C5 by oxidoreduction, and introducing the azido group with a second inversion. The

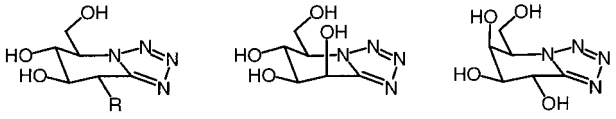

20 R = OH
23 R = NHAc

21 **22**

manno-, *galacto*-, and *N*-acetylglucosamine-derived tetrazoles **21**, **22**, and **23** were prepared similarly.[67, 68] More recently, we have transformed protected glyconolactams in one step to these and similar tetrazoles by treatment with sodium azide and trifluoromethanesulfone (triflic) anhydride.[69]

These tetrazoles are indeed half-chairs in D_2O. For **20** and **21**, a half-chair to sofa conformation has also been established by X-ray analysis (Figure 3). These tetrazoles possess an

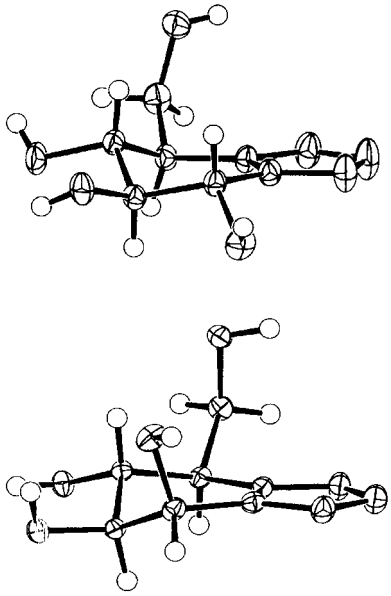

Figure 3. X-ray structures of **20** (top) and **21** (bottom).

excellent shelf life and are stable in solutions over a pH range of 1–14. Their inhibition of α- and β-glycosidases (Table 3) is similar to that of glucono-1,5-lactone **1** (Table 1) and of mannono-1,5-lactone (1.7 μM against snail β-mannosidase[70]).

To explore the question of their configurational selectivity, the inhibition by the *gluco*- and *manno*-tetrazoles **20** and **21** was tested by Withers et al. against three mannosidases and three glucosidases.[67] Each of these glucosidases and mannosidases hydrolyzes both glucosides and mannosides, though there is a much greater activity with the correct substrate, as quantified by $V_{max}K_M^{-1}$ values. Correspondingly, all these

Table 3. K_i values [μM] of the *gluco*- and *manno*-tetrazoles **20** and **21**.

Enzyme (source)	**20**	**21**
α-glucosidase (yeast)	1300	100000
β-glucosidase (almonds)	200	–
β-glucosidase (*Agrobacterium faecalis*)	1.4	6000
β-galactosidase (bovine liver)	1.5	14000
α-mannosidase (jack beans)	8500	180
α-mannosidase (almonds)	13800	700
β-mannosidase (snail)	47000	160

enzymes are inhibited by both tetrazoles, but the correct tetrazole is considerably more effective than the incorrect one. Thus, β-glucosidases are inhibited more strongly by **20** than by **21**, and the β-mannosidase more strongly by **21** than by **20**. There is some inhibition of the α-glycosidases, but only in the millimolar range; again, there is discrimination of the configuration at C2. This demonstrates the configurational selectivity of these glycosidases and inhibitors.

To settle the question of the transition state analogue character of the tetrazoles appeared all the more important since it had never been demonstrated for the glyconolactones. Two types of experiments were performed. First, the activation free energy ($V_{max}K_M^{-1}$) for each substrate and corresponding enzyme was plotted against the free energy of binding of the inhibitor (K_i^{-1}; Figure 4).[67] Rate enhancement

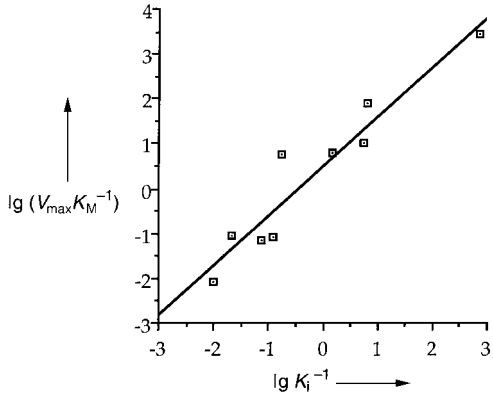

Figure 4. Plot of inhibition constants K_i of tetrazoles versus $V_{max}K_M^{-1}$ of the substrate.

for the transformation of the substrate reflects transition state binding of the substrate, and that should correspond to the binding of transition state analogue inhibitors, but not to ground state substrate binding. This plot for the binding of substrates and inhibitors to these enzymes is characterized by a slope of 1.1 and a correlation coefficient of $r = 0.9$, as expected for a transition state mimic, while there was no correlation with K_M. The good correlation obtained, despite the enzymes belonging to different families, must mean that the tetrazoles are complementary to a common aspect of the transition state structure of these enzymes.

Further evidence for the transition state character of the tetrazoles comes from studying a mutant of the *Agrobacterium faecalis* β-glucosidase where glutamic acid 358 has been replaced by aspartic acid.[71] Glutamic acid 358 is the catalytic nucleophile; thus it plays a major role in transition state binding, but a minimal one in ground state binding. This mutation results in a decrease in rate constants of about 10000-fold (corresponding to a $\Delta\Delta G$ value of ca. 5.6 kcal mol^{-1}), while the binding of substrate (ground state) analogues is weakened only 5-fold ($\Delta\Delta G$ ca. 1 kcal mol^{-1}) and of the gluco-tetrazole **20** some 200-fold ($\Delta\Delta G$ ca. 3.2 kcal mol^{-1}). These results show the tetrazole to be a transition state analogue, albeit an imperfect one. This finding may be extrapolated to glyconolactones, glyconolactams, and their oximes.

These experiments show that the configuration of the inhibitor is relatively unimportant only for transition state analogue inhibitors of configurationally unselective enzymes.

2.4. Enzymic Protonation of Inhibitors

2.4.1. C-Glucosyl Imidazoles

The inhibition of the sweet-almond β-glucosidases by several imidazole derivatives, such as 4-phenylimidazole, reported by Li et al. and Field et al.[72, 73] suggested that protonation by the enzyme is indeed important for the activity of glycosidase inhibitors. The inhibition by the imidazoles was readily interpreted on the basis of the generally accepted mechanism. Imidazoles may interact synergistically with an acid and a base (Figure 5a). According to molecular mechanics calculations, the imidazole ring of the C-glucosyl imidazole **27** should be more or less perpendicular to the plane of the pyranose ring. Thus, it should be ideally disposed to interact with the catalytic acid and the catalytic nucleophile, disposed on opposite sides of the average plane of the pyranose ring[74] (Figure 5b).

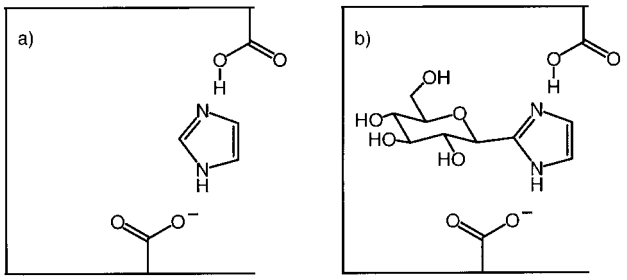

Figure 5. Mechanism of inhibition of glycosidases by imidazole (a) and β-D-glucopyranosylimidazole (b).

The C-glucosyl imidazoles **25** and **27** were made by addition of an N-protected 2-lithioimidazole to tetrabenzyl gluconolactone **14**, reduction of the resulting hemiacetal **24** to the diol, and selective acylation followed by base-promoted cyclization to **26**.[74] To our surprise, both the hemiacetal **25** and the

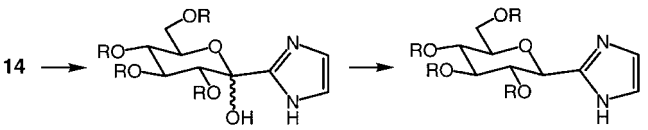

C-glycoside **27** turned out to be weak inhibitors of the β-glucosidases from sweet almonds (Table 4). Why? Which factor is responsible for the weak inhibition—conformation or the greater distance of the basic nitrogen atom from the anomeric center?[75, 76]

Table 4. K_i values [μM] of the *C*-glucosyl imidazoles **25** and **27**.

Enzyme (source)	**25**	**27**
β-glucosidase (almonds)	790	640

2.4.2. Annulated Pyrroles and Imidazoles

During our work on these inhibitors, Aoyagi, Aoyama, and co-workers published the structure of the natural product nagstatin (**28**), a very potent inhibitor of some glucosaminidases with a K_i value of 4 nM for the porcine kidney enzyme.[77, 78] Tatsuta et al. synthesized the *gluco*-, *manno*-, *galacto*-, and *talo*-imidazoles **31**, **32**, **33,** and **34** by addition of

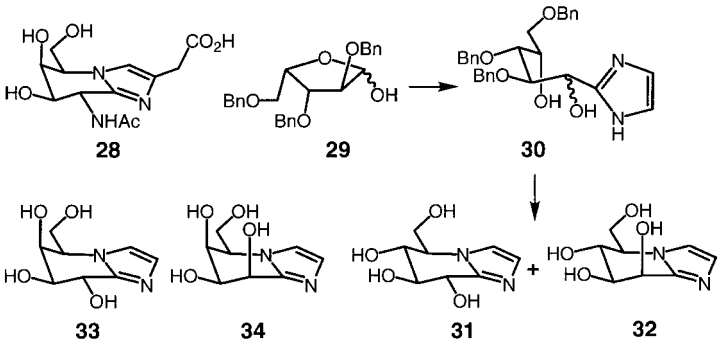

lithiated *N*-tritylimidazole to protected L-pentofuranoses, such as **29**, and cyclization of the resulting diastereoisomeric diols.[79–82] Although the IC_{50} values of these imidazoles were not determined under the same conditions as the K_i values of the tetrazoles, the imidazoles are clearly more potent inhibitors of β-glycosidases, and show little activity towards α-glycosidases (Table 5). Thus, the inhibitory activity of nagstatin is mainly associated with the imidazole ring and not with the carboxymethyl substituent.

Table 5. IC_{50} values [μM] of the annulated imidazoles **31**–**33**. Values in $\mu g\,mL^{-1}$ [80] have been transformed in μM.

Enzyme (source)	**31**	**32**	**33**
α-glucosidase (bakers' yeast)	105	> 500	> 500
β-glucosidase (almonds)	0.7	17.5	0.5
β-mannosidase (snail)	300	0.11	370
β-galactosidase (*E. coli*)	> 500	> 500	0.008

The tetrazole **20** and the imidazole **31** possess a very similar shape; hence, the imidazole ought also to be a transition state analogue. Transition state analogues should be protonated in the same way as the substrate on the way to the transition state. The Koshland–Phillips–Vernon mechanism implies that proton transfer from the catalytic acid to the inhibitor occurs in the π plane of the azole. This would lead to C-protonation of the imidazole (but hardly the tetrazole) and loss of aromaticity (Figure 6), as has been observed in

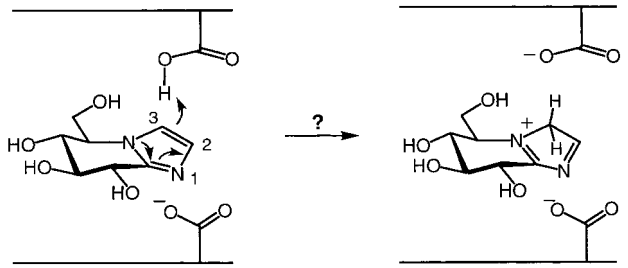

Figure 6. Application of Koshland's mechanism[23] to the inhibition of glycosidases by the annulated *gluco*-imidazole **31**.

histidine ammonia lyase.[83, 84] If this should be so, one expects the analogous pyrrole to be a stronger inhibitor than the imidazole.

The pyrroles **39** and **40** were prepared from the gluconolactam **17** that again proved its value as an advanced intermediate. The key step is the 1,3-dipolar cycloaddition

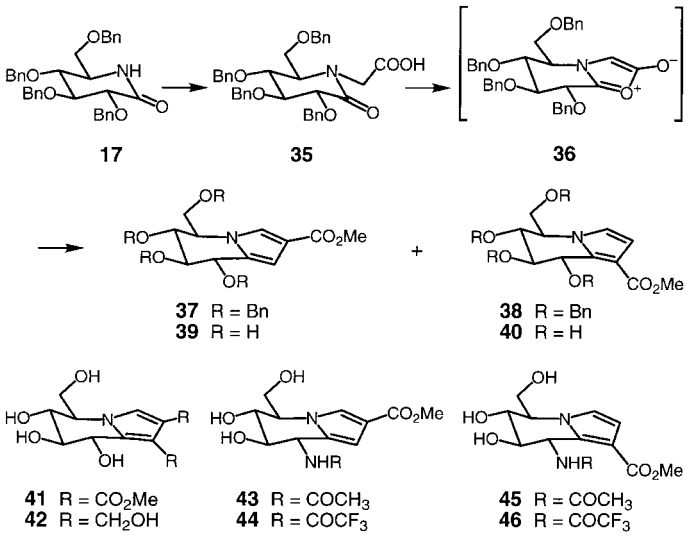

of the münchnone **36** to methyl propiolate.[85] Alkylation of the lactam **17** with ethyl iodoacetate, saponification, and dehydration of the substituted glycine **35** in the presence of propiolate gave the regioisomeric esters **39** and **40** in good yields. The deprotected pyrroles possess a half-chair conformation in solution and in the solid state (Figure 7). These compounds were very weak inhibitors, as were the analogous diester **41** and diol **42** derived from the cycloaddition of **36** to dimethyl acetylenedicarboxylate (Table 6). For the preparation of the analogous *N*-acetyl and *N*-trifluoroacetyl glucosamine-derived pyrroles **43**–**46**, we treated **37** and **38** with Me_3SiN_3 and a Lewis acid, introducing the azide group by regioselective elimination followed by addition to the intermediary azoniafulvenes.[86] The *N*-acetylglucosamine-derived pyrroles were moderately strong inhibitors of bovine β-*N*-acetylglucosaminidase, but, again, they were significantly weaker than the corresponding tetrazole (Table 7).

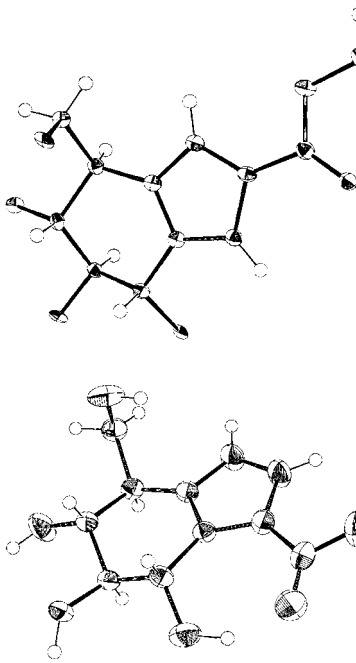

Figure 7. X-ray structures of **39** (top) and **40** (bottom).

Table 6. K_i values [μM] of the annulated pyrroles **39**–**42** derived from glucose.

Enzyme (source)	**39**	**40**	**41**	**42**
β-glucosidase (almonds)	6000	300	25000	14000

Table 7. K_i values [μM] of the annulated pyrroles **43**–**46** and the tetrazole **23** derived from GlcNAc.

Enzyme (source)	**43**	**44**	**45**	**46**	**23**
β-glucosaminidase (bovine kidney)	19	10	20	13	0.2

3. A Modified Hypothesis: In-Plane or "Lateral" Protonation

These results and the hypothesis that proton transfer to the inhibitor is important could only be reconciled by postulating that protonation of the substrate and of a transition state analogous inhibitor takes place in a different way from that generally assumed. According to the original interpretation of the X-ray analysis of crystalline lysozyme, the two catalytic carboxyl residues are located "on each side of the center of formal substitution";[24, 87] that is, the catalytic acid/base is above the mean plane of the pyranoside ring, and the nucleophile below it, as depicted in Figure 1a. This finding has tacitly been generalized to other β-glycosidases.[88]

The glycosidic oxygen atom has two doubly occupied nonbonding orbitals by which it can interact with a proton donor. In the preferred conformation (rationalized by the *exo* anomeric effect[89]), one of them is oriented more or less in the plane of the pyranoside ring, and the other perpendicular to it (Figure 8a). All lactone-type inhibitors possess a heteroatom corresponding to the glycosidic

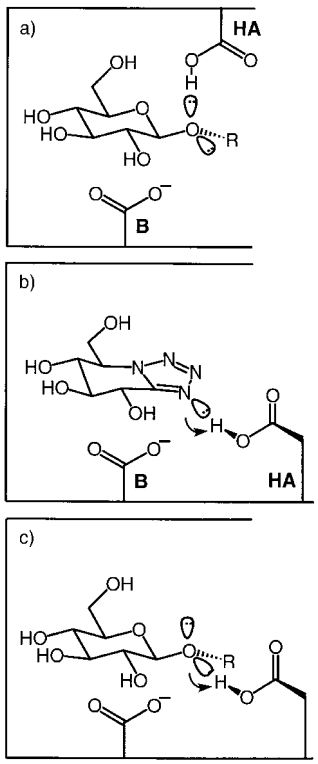

Figure 8. Proposed direction of protonation a) of a glucoside perpendicular to the plane of the ring and b) and c) of *gluco*-tetrazole **20** and a glucoside in the plane of the ring.

oxygen atom of the substrate. This heteroatom possesses a protonable lone pair only in the mean plane of the ring. Since proton transfer to the tetrazole **20** and related lactone-type inhibitors can only occur in the plane of the ring,[90] the same must be valid for the substrate; that is, the proton donor must be close to the mean plane of the ring, and not perpendicular to it (Figure 8b, c). This places the catalytic acid much closer to the catalytic nucleophile than would be possible if they were on opposite sides of the mean plane of the pyranose ring, in agreement with the effect of the formation of the intermediate glycosyl ester on the pK_a value of the catalytic acid.[91]

3.1. Synthesis of Annulated 1,2,3-Triazoles

To confirm the hypothesis of in-plane protonation we decided to compare the inhibition of β-glycosidases by the tetrazole **20** with that by the analogous 1,2,3-triazole **47**. The 1,2,3-triazole must possess a very similar shape to the tetrazole, but proton transfer is no longer possible as the position corresponding to the glycosidic oxygen is occupied by a CH group.

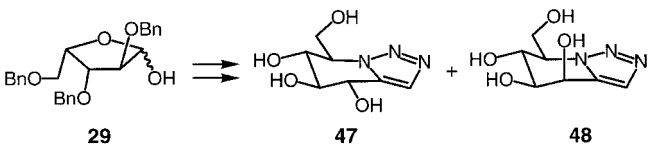

29 **47** **48**

The *gluco*- and *manno*-1,2,3-triazoles **47** and **48** were prepared by intramolecular 1,3-dipolar cycloaddition of azidoalkynes, which are readily available from the tri-*O*-benzyl-L-xylose **29** by addition of an alkynyl cerium, regioselective protection, and substitution at C5 with azide.[92] The benzylated *gluco*- and *manno*-1,2,3-triazoles were readily separated and deprotected to **47** and **48**.

These triazoles possess very similar conformations to their tetrazole analogues, both in solution and, for **47**, in the solid state (Figure 9), but a dramatically different inhibitory

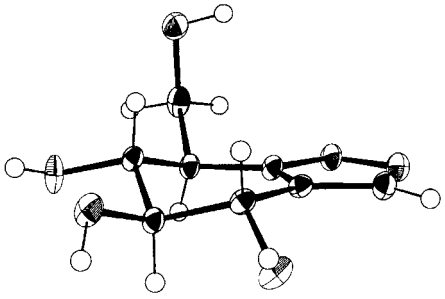

Figure 9. X-ray structure of **47**.

potency (Table 8). The triazole **47** is inactive at a concentration of 8 mM against the β-glycosidases from sweet almonds and bovine liver, and against the β-glucosidase from *C. saccharolyticum* it is 400 times weaker than the tetrazole **20**. The *manno*-triazole **48** is inactive at 8 mM against snail β-mannosidase. This is equivalent to a loss of binding energy of 3.3 – 5.0 kcal mol^{-1}, in keeping with the hypothesis of a lateral protonation at N1 of the tetrazole **20**.

Table 8. IC_{50} values [μM] of the *gluco*- and *manno*-tetrazoles **20** and **21** and the *gluco*- and *manno*-1,2,3-triazoles **47** and **48**.

Enzyme (source)	**20**	**47**	**21**	**48**
β-glucosidase (almonds)	200	> 8000	–	–
β-glucosidase (*Caldocellum saccharolyticum*)	5	2000	–	–
β-mannosidase (snail)	–	–	150	> 8000
β-galactosidase (bovine liver)	1.5	> 8000	–	–

3.2. Hydrogen Bonding versus Charge – Charge and Charge – Dipole Interactions

The in-plane protonation explains the difference between the inhibition of the tetrazole and 1,2,3-triazole. It does not, however, explain why Ganem's dimethylamidinium salt **49**, which cannot form a hydrogen bond in the plane of the ring (Figure 10a), with a K_i value of 83 μM against the sweet-almond β-glucosidases[58] is about as good an inhibitor as the tetrazole **20** ($K_i = 150$ μM[67]). The binding of **49** must be favored by a charge – charge interaction with the catalytic nucleophile, which suggests an analogous charge – dipole interaction for neutral lactone analogues (Figure 10b). This recalls the explanation by Reese et al. for the inhibition by glyconolactones, that is, the interaction between the negative charge of the catalytic nucleophile and the dipole of the C=O bond.[39] This charge – dipole interaction is consistent with the stronger inhibition by the more electronegative tetrazole as compared with the 1,2,3-triazole.

Conceivably, the importance of this charge – dipole interaction might be investigated by systematically modifying the number and position of the nitrogen atoms in the azole ring. For the in-plane (i.e., "lateral") protonation one expects a correlation between inhibitory power and basicity of the azole. The inhibitory power should thus increase in the series tetrazole < 1,2,4-triazole < imidazole. If the charge – dipole interaction were decisive, the tetrazole should be the strongest and the imidazole the weakest inhibitor. However, the two factors—protonation and the interaction with the catalytic nucleo-

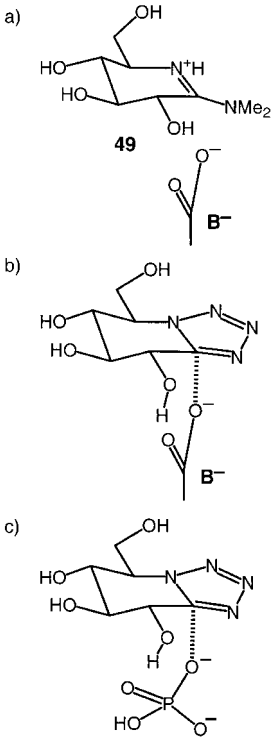

Figure 10. Charge – charge or charge – dipole interaction in β-glycosidases between the catalytic nucleophile and a) the amidinium ion **49** or b) the *gluco*-tetrazole **20** and c) in glycogen phosphorylase b between the catalytic nucleophile and the *gluco*-tetrazole **20**.

phile—are not independent of each other. Progressive proton transfer to the azole in theory leads ultimately to an azolium cation, and thereby to a salt bridge and a charge–charge interaction with the catalytic nucleophile that should be stronger than any charge–dipole interaction, although the expected small pH difference between the catalytic acid and the imidazole, both around pH 7, makes a complete proton transfer unlikely, even considering the favorable entropic effects.[93, 94] To evaluate the contribution of the charge–dipole interaction independently from a (partial) proton transfer, we considered using the known interaction of hydrogen phosphate or dihydrogen phosphate with the tetrazole **20** in glycogen phosphorylase b[95] (Figure 10c), which lacks a catalytic acid in the active site.[96, 97] We will return to these questions after discussing the inhibition of the β-glycosidases by the various azoles.

3.3. Annulated 1,2,4-Triazoles and Imidazoles: Synthesis and Inhibition

As mentioned in Section 2.4.2, the inhibition of the imidazole **31**[79] and the tetrazole **20** was measured under different conditions. To allow a valid comparison, we devised a new synthesis of the imidazoles **31** and **32** and the 1,2,4-triazoles **51** and **53**.

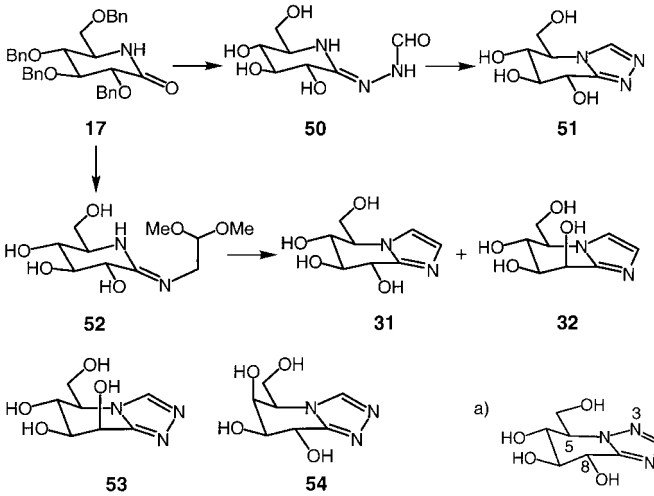

The gluconolactam **17** again served as an advanced common intermediate. Conversion into the thionolactam **18**, addition of *N*-formylhydrazine, cyclization under acidic conditions, and deprotection gave the 1,2,4-triazole **51** in 49% yield (from **17**).[98] The use of aminoacetaldehyde dimethyl acetal in place of formylhydrazine yielded the amidine **52**, which was cyclized under acidic conditions to give, after deprotection, the *gluco*- and *manno*-imidazoles **31** and **32** (60% from **17**).[98] The *galacto*-imidazole **33** (see Section 2.4.2) was prepared similarly in 60% yield from tetra-*O*-benzyl-1,5-gal-actonolactam.[99] These 1,2,4-triazoles and imidazoles possess very similar conformations to the 1,2,3-triazoles and tetrazoles in solution and, for the hydrochloride of **31**, in the solid state (Figure 11).

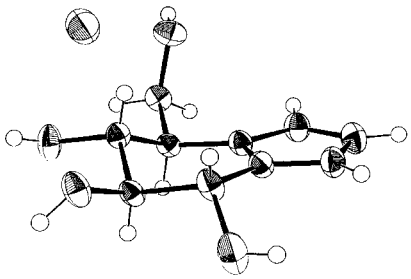

Figure 11. X-ray structure of **31** · HCl.

Tatsuta et al. had previously synthesized the *manno*- and *galacto*-1,2,4-triazoles **53** (27% yield from 2,3,5-tri-O-benzyl-L-xylose) and **54** (24% yield from 2,3,5-tri-O-benzyl L-ribose) using lithiated azoles that allowed rapid access to the imidazoles **31**/**32** and **33**/**34**.[100]

Among the *gluco*-, *manno*-, and *galacto*-azoles, the imidazoles proved consistently stronger β-glycosidase inhibitors than the 1,2,4-triazoles, which, in turn, are stronger inhibitors than the tetrazoles. The K_i values reported in Figure 12 are consistent with the dominant influence of the proposed in-plane protonation.

3.4. Glycogen Phosphorylase: Further Clues to Inhibitor Binding in Glycosidases

As mentioned in Section 3.2, the contribution to the inhibition of the charge–dipole interaction between the azole and the catalytic nucleophile B^- might be quantified by studying glycogen phosphorylase b (GP*b*). GP*b* phosphorolytically cleaves the α-glycosidic bonds of glycogen, but in contrast to the glycosidases possesses no catalytic proton

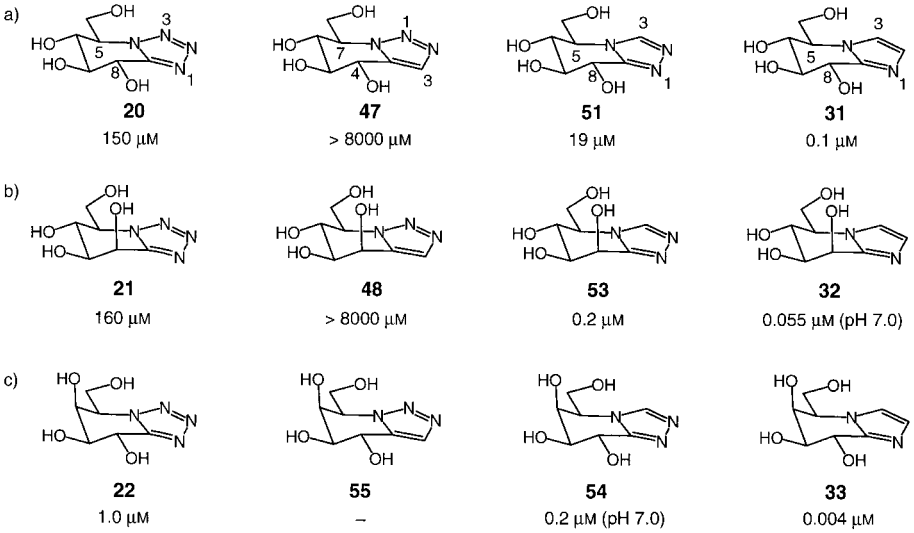

Figure 12. K_i values of *gluco*-, *manno*-, and *galacto*-configured tetrahydropyridoazoles against a) almond β-glucosidase, b) snail β-mannosidase, and c) *E. coli* β-galactosidase.

donor; both the function of the catalytic proton donor and of the catalytic nucleophile are performed by hydrogen phosphate or dihydrogen phosphate.[96, 97] It had been found[95] that the tetrazole **20** inhibits GP*b* ten times more strongly in the presence of phosphate than in its absence. An X-ray structure of the GP*b* – phosphate – tetrazole complex showed that the hydrogen phosphate or dihydrogen phosphate ion is located beneath the inhibitor, with the proximal oxygen atom 3.1 Å removed from the "anomeric" carbon atom[95] (see Figure 10c), presumably interacting with the azole ring by a charge – dipole interaction. The position of the hydrogen phosphate or dihydrogen phosphate ion with respect to the tetrazole strongly resembles that expected for the catalytic carboxylate in β-glycosidases (see Figures 1, 10b, and 10c). In GP*b*, however, there is no hydrogen bond to the nitrogen atom of the tetrazole corresponding to the glycosidic oxygen atom. These properties make GP*b* a suitable model to investigate the interaction between an anion corresponding to the catalytic nucleophile and the tetrazole **20**, or the 1,2,3-triazole **47**, without any interference from protonation of the azole.

In the presence of phosphate, the 1,2,3-triazole **47** binds ten times more weakly to GP*b* than the tetrazole **20**, which is equivalent to a difference in binding energy of about 1.4 kcal mol^{-1} at 25 °C (Table 9). A comparison of the crystal

Table 9. K_i values [μM] of tetrazole **20**, the 1,2,4-triazole **51**, the 1,2,3-triazole **47**, and the imidazole **31** against almond β-glucosidase and glycogen phosphorylase b (GP*b*).

Inhibitor	K_i (β-glucosidase), mode of inhibition	K_i (GP*b*/phosphate), mode of inhibition	K_i (GP*b*/Glc-1-*P*), mode of inhibition
20	150, competitive	53, competitive	700, competitive
51	19, competitive	8100, competitive	no inhibition[a]
47	> 8000, no inhibition	540, competitive	2500, competitive
31	0.35, competitive	9700, competitive	no inhibition[a]

[a] At concentrations of inhibitors from 0.1 to 5 mM in the presence of 3 mM Glc-1-*P*, 1 mM AMP, and 1% glycogen.

structure of the GP*b* – phosphate – triazole and GP*b* – phosphate – tetrazole complexes shows that (within the resolution limits) the tetrazole **20** and triazole **47** are bound in the same way (Figure 13). Thus the strength of the interaction between the azole and the hydrogen phosphate or dihydrogen phosphate must be the dominant factor contributing to the difference in binding energy.[101]

The 1,2,4-triazole **51** and imidazole **31** are not bound significantly at the active site of GP*b* (Table 9). The structure of the ternary complexes of the tetrazole or triazole indicates that replacement of N3 of the tetrazole by CH must interrupt a hydrogen bond with an enzymic main chain NH group (Leu 136), thus lowering the binding affinity (see Figure 13). Hence, the evaluation of the oxyanion – azole interaction with the phosphate ion had to be restricted to **20** and **47**.

The relatively small difference in binding energy for the tetrazole **20** and 1,2,3-triazole **47** to GP*b* suggests that the oxyanion – azole interaction is not the main factor responsible for the large difference in binding energy of these azoles to β-glycosidases. However, for β-glycosidases one expects partial protonation of the azoles to raise their electronegativity, and

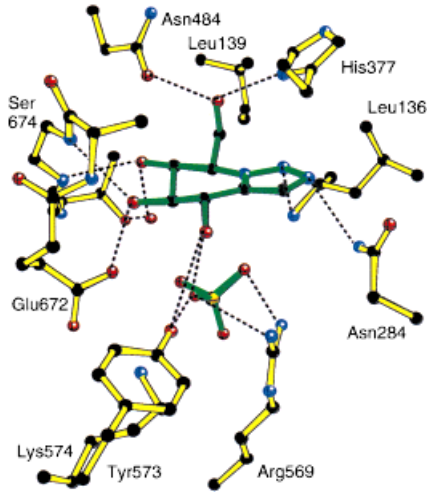

Figure 13. Structure of the complex made up of GP*b*, 1,2,3-triazole **47**, and phosphate.

to increase the strength of the interaction of the azole (or azolium cation) with the catalytic nucleophile; the two interactions—protonation and interaction with the catalytic nucleophile—should be synergistic. The synergism, expressed in Figure 8b, means that the individual contributions to the inhibition of the lateral protonation and of the interaction with the catalytic nucleophile are not experimentally accessible. However, the experimental difference for the interaction between phosphate and the 1,2,3-triazole **47** or the tetrazole **20** in the active site of GP*b* may be used to validate semiempirical (AM1) calculations of this energy difference, which may then be extended with reasonable confidence to quantify the interaction between the azole inhibitors and the catalytic nucleophile of β-glycosidases.

The interaction between the gluconotetrazole **20**, the 1,2,3-triazole **47**, the 1,2,4-triazole **51** or the imidazole **31**, and either hydrogen phosphate or dihydrogen phosphate was determined by calculating a range of heats of formation for each complex, reducing the distance between the proximal phosphate oxygen atom and the "anomeric" carbon atom by increments of 0.1 Å to give a potential energy curve.[101] As shown in Figure 14, the oxyanion – azole interaction for either a hydrogen phosphate or dihydrogen phosphate ion increases with the number of nitrogen atoms in the azole ring (i.e., it correlates inversely with the energy of the LUMO). The ΔK_i-derived energy difference for the phosphate – tetrazole and phosphate – 1,2,3-triazole interaction in GP*b* (1.4 kcal mol^{-1}) and the crystallographic data agree with the calculated difference between the energy minima (ΔE_{min}) of 1.1 kcal mol^{-1} and the geometry for the complexes with the dihydrogen phosphate rather than with the hydrogen phosphate ion. On the basis of this close correspondence, we similarly calculated the heats of formation for the azole – carboxylate complexes, maintaining the conformation of the HO group at C2 that is required for the important hydrogen bond[102] between this group and the catalytic nucleophile. A similar dependence of the energy of interaction and the number of nitrogen atoms of the azoles was observed, as before (Figure 14), with a calculated energy difference of

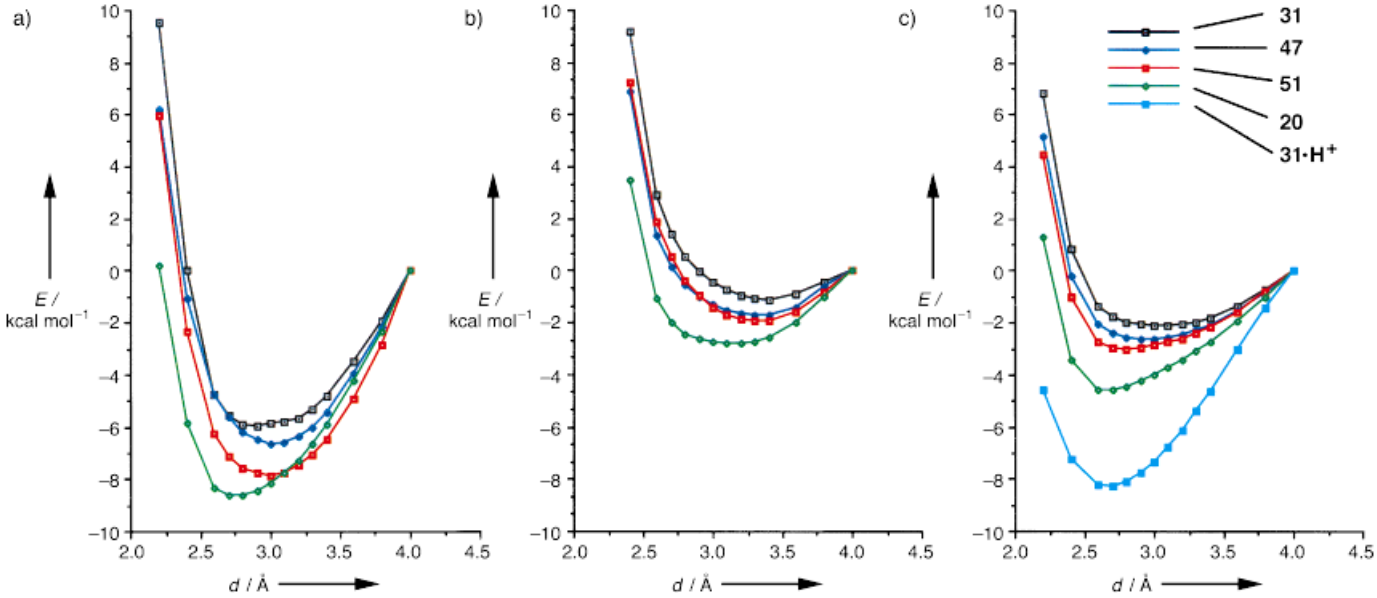

Figure 14. Results of AM1 calculations: plots of potential energy E versus the distance d between the oxygen atom of a) HPO_4^{2-}, b) $H_2PO_4^-$, and c) $CH_3CO_2^-$ and the "anomeric" carbon atom of the azole inhibitors **20**, **51**, **47**, and **31**.

2.0 kcal mol^{-1} for the tetrazole and 1,2,3-triazole complexes. This compares to an experimental difference of binding energy between **20** or **47** and the β-glycosidases listed in Table 8 of at least[103] 2.4 to 5.3 kcal mol^{-1}. This means that the interaction with the catalytic nucleophile contributes only about half of the binding energy; the other half must derive from the interaction with the catalytic acid.

The strength of the calculated azole – oxyanion interaction correlates with the inhibition of GP*b*, but with a trend that is opposite for the inhibition of β-glycosidases by these azoles. In agreement with the synergism between the two interactions, the calculations showed that protonation of the imidazole **31** dramatically increases the energy of the interaction with the catalytic nucleophile, by as much as 6 kcal mol^{-1}.

3.5. Insights from X-ray Structures and Molecular Modeling

3.5.1. In-Plane Protonation

The hypothesis of in-plane protonation was initially checked by docking the *gluco*- and *galacto*-tetrazoles **20** and **22** into the active site of the three configuration-retaining *exo*-β-glycosidases, for which structures were then available from X-ray analysis.[92] Two features facilitated docking of the inhibitors. Firstly, *exo*-enzymes cleave the terminal pyranoside residue from the nonreducing end of an oligosaccharide or glycoside, so the fissile glycosidic bond must point towards the entrance of the binding pocket. Secondly, the catalytic nucleophile must be located on the α face of the pyranoside ring, about 3 Å beneath the anomeric carbon in a position to attack the incipient oxycarbenium ion.

Although belonging to two different families according to Henrissat's amino acid sequence classification,[51, 52] the *E. coli* β-galactosidase (family 2),[104] white clover cyanogenic β-glucosidase,[105] and *L. lactis* 6-phospho-β-galactosidase (both family 1)[106] show very similar arrangements of polar and hydrophobic side chains in their active sites. Additional information relevant to the docking of inhibitors into these glycosidases was provided by the structure of a *Cellulomonas fimi* cellulase by White et al.[107] Although it is an *endo*-glycosidase, and belongs to family 10, the arrangement of amino acid side chains responsible for recognition of the pyranoside ring and for catalysis is very similar to that in the active site of the above three *exo*-glycosidases. In the *C. fimi* cellulase structure, the catalytic nucleophile is covalently bonded to a 2-deoxy-2-fluorocellobiosyl moiety (Figure 15), which strongly supports the long-standing hypothesis that, at least in some glycosidases, hydrolysis proceeds via a glycosyl ester.[23, 108]

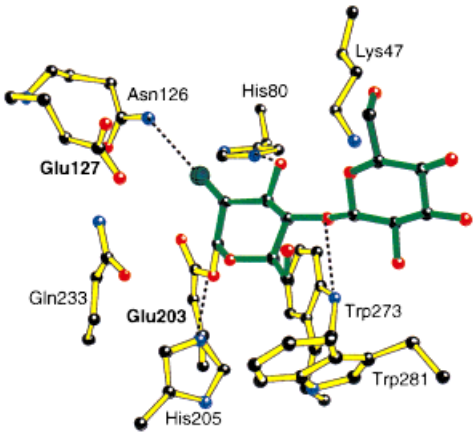

Figure 15. Structure of *C. fimi* endocellulase (family 10) covalently bonded to a 2-deoxy-2-fluoro-cellobiosyl moiety.[107]

The structures which resulted from manual docking of the tetrazoles **20** or **22** into the active site of the three *exo*-glycosidases are strikingly similar (Figure 16a – c).[92] Energy minimization, using fixed enzyme coordinates and starting from the geometry of the complexes resulting from manual

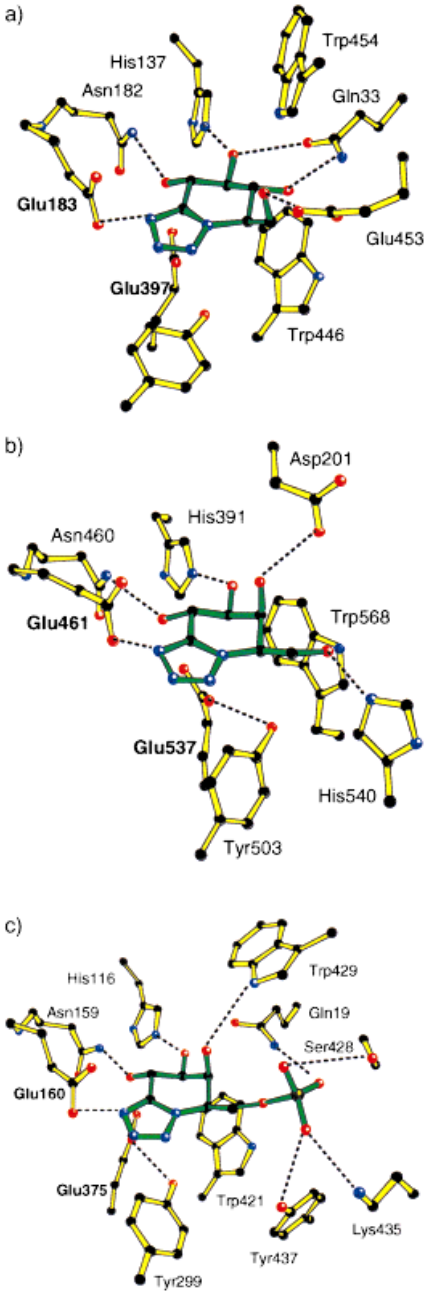

Figure 16. Modeled structures of complexes a) between *E. coli* β-galactosidase (family 2) and *galacto*-tetrazole **22**, b) between white-clover β-glucosidase (family 1) and *gluco*-tetrazole **20**, and c) between *L. lactis* 6-phospho-β-galactosidase (family 1) and phosphate derived from *galacto*-tetrazole **22**.[92]

docking, suggested that the resulting geometry reflects the optimal inhibitor binding orientation. Potential hydrogen bonds are observed between the glycosidic heteroatom and the carboxyl group of the conserved catalytic acid Glu, between HO-C2 and the conserved Asn preceding the catalytic acid, and between HO-C3 and a conserved His. The models also indicate a hydrophobic stacking at the α face, between the pyranoside ring and a conserved Trp residue, typical in carbohydrate-binding proteins.[109] The inescapable conclusion is that the catalytic proton donor is indeed located close to the mean plane of the pyranoside ring; rotation of the inhibitor, or movement of the catalytic proton donor, so that protonation could occur from above the ring is unfeasible. Sakon, Karplus et al. determined the structure of a cellotetraose substrate bound to the active site of a family 5 endocellulase, in which they observed a very similar array of hydrogen bonds and hydrophobic interactions (Figure 17a).[110] The authors commented that the location of the catalytic groups with respect to the fissile glycosidic bond

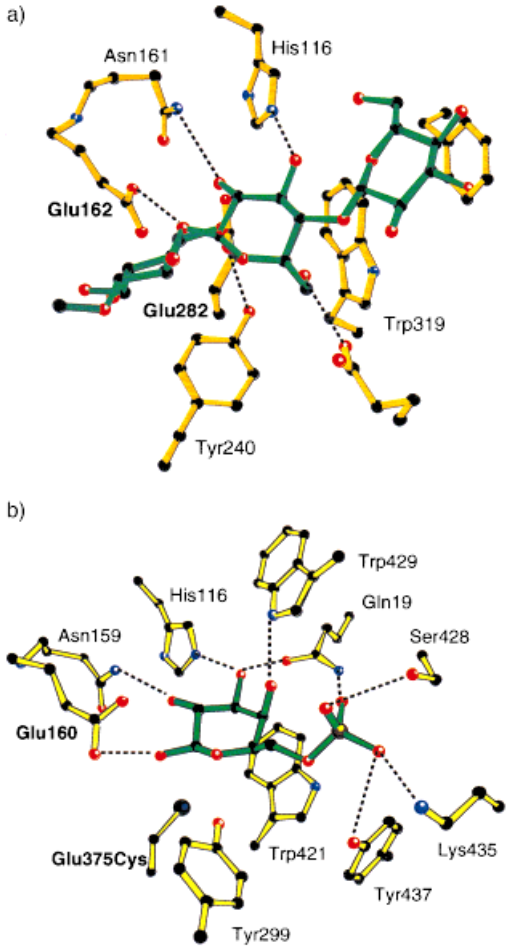

Figure 17. Structures of complexes between a) *A. cellulolyticus* endocellulase (family 5)[110] and substrate and b) *L. lactis* 6-phospho-β-galactosidase (family 1)[111] and product.

contrasts with the "textbook paradigm" since these groups are not on opposite sides of the glycon ring plane, but the proton donor is located close to the mean plane of the pyranoside ring and close to the catalytic nucleophile. Wiesmann et al. subsequently determined the crystal structure of a mutant of 6-phospho-β-galactosidase complexed with 6-phospho-β-galactose[111] (Figure 17b), confirming all the interactions proposed in our inhibitor model[92] and again showing that the proton donor is located close to the ring plane.

3.5.2. Generality of In-Plane Protonation—Classification of Glycosidases according to the syn or anti Protonation Trajectory

In-plane protonation thus appeared fairly well established, at least for the β-glycosidases we had examined. This raises the question of whether in-plane protonation is a general feature of glycosidases.

There is now a significant body of data available from crystal structure analyses of configuration-retaining β-glycosidases complexed with substrates, products, or inhibitors.[104, 105, 107, 110–144] In all of the complexes, the proton donor is located close to the mean plane of the pyranoside ring of the substrate or an inhibitor (Table 10). These structural data also reveal that there are two types of β-glycosidases. In the first type, the proton donor is *anti* to the pyranoside ring oxygen atom with respect to the plane defined by O1, C1, and H1, as in the structures described above (i.e., *anti* to the (C5)O–C1 bond; Figure 18a). This corresponds to the orientation of one of the doubly occupied, nonbonding orbitals on the glycosidic oxygen atom when the aglycon is in the orientation favored by the *exo* anomeric effect. In the second type, the proton donor is located *syn* to the ring oxygen atom, requiring a conformation which is not favored by the *exo* anomeric effect (Figure 18b). Table 10 shows the considerable number of glycosidase structures which are compatible with an *anti* or *syn* in-plane protonation trajectory. A small number of glycosidases do not show sufficient structural homology to assign them as *anti* or *syn* protonators. Their assignment will be assisted by the analysis of crystalline ligand complexes.

There is, perhaps unsurprisingly, a correlation between the glycosidase families[51, 52] defined by the amino acid sequence and the *syn* or *anti* protonation trajectory. The similarity of the structure of the active site for enzymes of families 1, 2, 5, and 10,[56, 104, 105, 107, 110, 112, 113, 119, 120, 122] which all belong to the GH-A clan, defines them as *anti* protonators. A similar *anti* orientation is also observed in a family 20 chitobiase;[118] *syn* protonators are found in families 7, 9, 11, 22, 23, and 45.[123, 125, 127, 129, 130, 145]

Table 10. Classification of glycosyl hydrolases according to *anti* or *syn* protonation trajectory.

Enzyme	Source	Conf.[e]	Family	PDB code	Ligand	Acid/base[a]	Nucleophile[a]	Ref.
***anti* protonators**								
6-phospho-β-galactosidase	*Lactococcus lactis*	$\beta-\beta$	1	4pbg	product	Glu160	Glu375	[111]
myrosinase	*Sinalpa albis*	$\beta-\beta$	1	2myr	2-F-glycosyl[f]	Gln187[b]	Glu409	[112]
cellulase C	*Clostridium thermocellum*	$\beta-\beta$	5	1cen	product	Glu140	Glu280	[113]
cellulase	*Acidothermus cellulolyticus*	$\beta-\beta$	5	1ece	substrate	Glu162	Glu282	[110]
cellulase	*Bacillus agaradherans*	$\beta-\beta$	5	–	2-F-glycosyl	?	?	
cellulase	*Cellulomonas fimi*	$\beta-\beta$	10	1exp	2-F-glycosyl	Glu127	Glu233	[107]
amylase I	porcine pancreas	$\alpha-\alpha$	13	1ppi	acarbose	Glu233	Asp197	[114]
amylase II	porcine pancreas	$\alpha-\alpha$	13	1ose	acarbose	Glu233	Asp197	[115]
amylase	*Aspergillus oryzae*	$\alpha-\alpha$	13	7taa	acarbose	Glu230	Asp206	[116]
CGTase[g]	*Bacillus circulans*	$\alpha-\alpha$	13	1cxg	acarbose	Glu257	Asp229	[117]
chitobiase	*Serratia marcescens*	$\beta-\beta$	20	1qbb	product	Glu540	–[c]	[118]
***anti* by similarity** (in amino acid sequence)								
β-glucosidase	white clover	$\beta-\beta$	1	1cbg	–	Glu183	Glu397	[105]
β-glycosidase	*Sulfolobus solfataricus*	$\beta-\beta$	1	1gow	–	Glu206	Glu387	[119]
β-galactosidase	*Escherichia coli*	$\beta-\beta$	2	1bgl	–	Glu461	Glu537	[104]
β-glucuronidase	human	$\beta-\beta$	2	1bhg	–	Glu451	Glu540	[120]
xylanase	*Clostridium thermocellum*	$\beta-\beta$	10	1xyz	–	Glu645	Glu754	[121]
xylanase A	*Pseudomonas fluorescens*	$\beta-\beta$	10	1clx	–	Glu127	Glu246	[122]
***syn* protonators**								
cellulase	*Fusarium oxysporum*	$\beta-\beta$	7	1ovw	thioglycosides	Glu202	Glu197	[123]
cellulase	*Thermonospora fusca*	$\beta-\alpha$	9	3tf4, 4tf4	product	Glu424	Asp55, Asp58	[124]
xylanase	*Bacillus circulans*	$\beta-\beta$	11	1bcx, 1xnb	substrate	Glu172	Glu78	[125]
lysozyme	hen egg white	$\beta-\beta$	22	1lyz, 9lyz, 1lsz	substrate	Glu35	Asp52	[126–128]
lysozyme	goose egg white	$\beta-\beta$	23	154l	substrate	Glu73	–[c]	[129]
endoglucanase V	*Humicola insolens*	$\beta-\alpha$	45	4eng	product	Asp121	Asp10	[130]
***syn* by similarity** (in amino acid sequence)								
cellobiohydrolase I	*Trichoderma reesei*	$\beta-\beta$	7	1cel	product	Glu217	Glu212	[131]
endoglucanase	*Trichoderma reesei*	$\beta-\beta$	7	1eg1	–	Glu201	Glu196	[132]
cellulase D	*Clostridium thermocellum*	$\beta-\alpha$	9	1clc	–	Glu555	Asp201	[133]
xylanase I	*Trichoderma reesei*	$\beta-\beta$	11	1xyn	-	Glu164	Glu75	[134]
xylanase II	*Trichoderma reesei*	$\beta-\beta$	11	1red, 1ree, 1ref	epoxyalkylglycosides	Glu177	Glu86	[135]
1,3–1,4-glucanase	*Bacillus macerans*	$\beta-\beta$	16	1byh, 1gbg	–	Glu109	Glu105	[136]
1,3–1,4-glucanase	*Bacillus macerans*	$\beta-\beta$	16	1mac	–	Glu107	Glu103	[137]
chitinase A	*Serratia marcescens*	$\beta-\beta$	18	1ctn	–	Glu315	Asp391	[138]
endochitinase	*Hordeum vulgare*	$\beta-\alpha$	19	2baa	-	Glu67	Glu89	[139]
unclassified								
cellobiohydrolase II	*Trichoderma reesei*	$\beta-\alpha$	6	1cb2	–	Asp221	Asp263	[140]
cellulase A	*Clostridium thermocellum*	$\beta-\alpha$	8	1cem	–	Glu95	Asp152	[141]
xylanase	*Streptomyces lividans*	$\beta-\beta$	10	1xas[d]	–	Glu128	Glu236	[142]
1,3–1,4-glucanase	*Hordeum vulgare*	$\beta-\beta$	17	1ghr	–	Glu288, Glu280	Glu232	[143]
endochitinase H	*Streptomyces plicatus*	$\beta-\beta$	18	1edt	–	Glu132	Asp130	[144]

[a] Acid/base and nucleophile assignments are taken from the accompanying references and in some cases may not be unambiguous. [b] Myrosinase has no catalytic proton donor; Gln187 occupies the same position as the isosteric, catalytic Glu in other family 1 glycosidases. [c] The *N*-acetamido group of the substrate acts as the nucleophile. [d] The PDB file gives only the coordinates of the peptide backbone. [e] Anomeric configuration of substrate and product. [f] Covalently bound 2-deoxy-2-fluoro substrate. [g] CGTase = cyclodextrin glycosyltransferase.

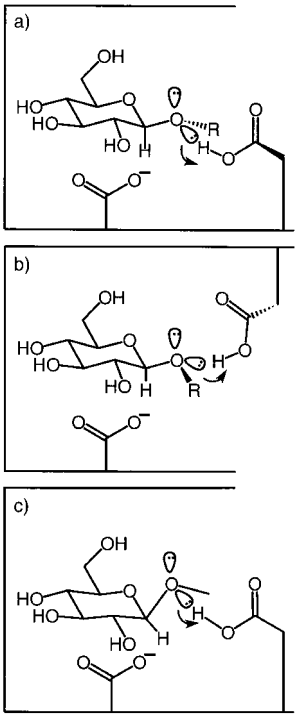

Figure 18. a) *anti* Protonation and b) *syn* protonation of a β-glycosidase; c) lateral protonation moves the fissile C–O bond into a pseudoaxial position.

Neither of these protonation trajectories corresponds to the lysozyme paradigm in which the catalytic residues were proposed to be located on "opposite sides" of the fissile glycosidic bond.[24, 25] However, recent high-resolution crystal structure analyses of inhibitor complexes show that lysozyme is a *syn* in-plane protonator.[128, 129] We have found no example of a configuration-retaining β-glycosidase in which the proton donor is not either *anti*- or *syn*-periplanar to the ring oxygen atom with respect to the above-defined plane.

It makes sense that the catalytic carboxy group is located close to the mean plane of the pyranoside ring and not above it. The departure of the aglycon in a pseudoaxial direction would be restricted if the carboxy group were located above the plane of the ring (Figure 18c). Stereoelectronic considerations, as expounded by Deslongchamps,[143] require that protonation of the glycosidic oxygen atom be accompanied by a lengthening of the fissile C–O bond in a pseudoaxial direction as the incipient oxycarbenium ion develops. This is supported by two high-resolution crystal structures of the cellulases from *Fusarium oxysporum*[123] (family 7, *syn* protonation; Figure 19) and *Bacillus agaradherans*[147] (family 5, *anti* protonation) by Davies and co-workers. They show that the pyranoside ring is distorted to a skew conformation which places the glycosidic bond in a pseudoaxial orientation. A similar observation has been reported for two chitin-degrading enzymes of families 18 and 20 by Tews et al.[148] Similarly, the water molecule which subsequently attacks the glycosyl ester intermediate must have access from the pseudoaxial direction.

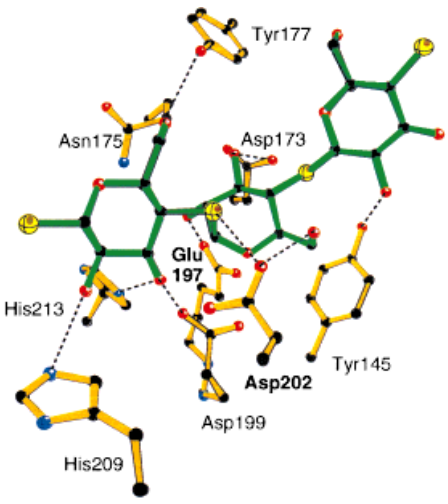

Figure 19. Structure of the complex between *F. oxysporum* cellobiohydrolase (family 7) and a thioglycoside.

The *syn* and *anti* protonation trajectories provide an important criterion for the design of selective inhibitors. Among the lactone-type inhibitors, only the lactone itself possesses a lone pair in a position suitable to accept a hydrogen bond from a *syn*-protonating catalytic acid; such a protonation is blocked in the azole inhibitors and in the hydroximolactams, which should be selective inhibitors of *anti*-protonating glycosidases. The testing of this hypothesis and the design and synthesis of selective inhibitors of *syn*-protonating glycosidases are in progress.

3.5.3. Configurational Selectivity

3.5.3.1. Inhibition of α- and β-Glycosidases

The results discussed in Section 3.5.2 indicate that the transition state for glycoside hydrolysis is characterized by a pseudoaxial orientation of the fissile C–O bond and a skew conformation. This appears to counter the evidence that lactone-type inhibitors are transition state analogues, since, in the ground state conformation, the carbonyl group accepting the hydrogen bond from the catalytic acid is in a pseudoequatorial orientation. However, it is not clear to what extent partial protonation and interaction with the catalytic nucleophile of a lactone or some of the lactone analogues will lead to rehybridization and to a change of conformation in the enzyme active site, so that the heteroatom attached to C1 is placed above the mean ring plane as shown in Figure 18c. Certainly, lactones easily adopt a boat or skew-boat conformation.[149] It seems likely, however, that lactone-type inhibitors mimic a structure corresponding to an early region of the reaction coordinate.

The active sites of configuration-retaining α- and β-glycosidases show similar locations for the hydrophilic and hydrophobic amino acid side chains responsible for recognition of the pyranoside ring. This suggests that the main differences between the two enzyme classes are the positioning of the catalytic nucleophile and of the catalytic proton donor. The catalytic nucleophile is for obvious reasons located close to the α face of the pyranoside ring in β-glycosidases, and to the β face in α-glycosidases. As discussed above, the proton donor is located in a plane close to the pyranoside ring plane in β-glycosidases; in α-glycosidases of family 13 (*anti* protonators) the proton donor is also to one side of the fissile bond, but in a plane about 1 Å below that of the mean ring plane,[114, 115, 150] corresponding to the position of the α-glycosidic oxygen atom.

As discussed in Sections 3.1–3.4 lactone-type inhibitors may be bound by a hydrogen bond with the catalytic proton donor, by a charge–charge (or charge–dipole) interaction with the catalytic nucleophile, or by a combination of these. Permanently protonated analogues such as the amidine **11** and the amidrazone **12** (see Section 2.2) are bound by charge–charge interactions, which are strong and relatively non-directional and may allow (minor) adjustments of the

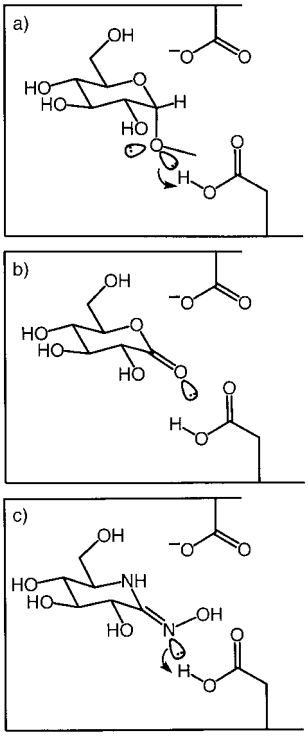

Figure 20. Interaction of the catalytic acid of α-glycosidases with a) an α-glycoside, b) the gluconolactone **1**, and c) the lactam oxime **13**.

binding geometry, consistent with their inhibition of both α- and β-glycosidases. By contrast, the selectivity in the inhibition of β- over α-glycosidases by neutral lactone-type inhibitors correlates with the directionality of the hydrogen bond, requiring an optimal positioning of the glycosidic heteroatom relative to the catalytic acid. In α-glycosidases neither the distance between the catalytic acid and the "glycosidic" heteroatom of neutral lactone-type inhibitors nor the orientation of these groups favor a strong hydrogen bond (Figure 20a, b). Is it possible to counter the energetic penalty of the geometric adjustment required for the inhibition of α-glycosidases by lactone-type inhibitors by increasing the strength of the hydrogen bond to the catalytic acid, that is, by using more strongly basic lactone analogues? It appears to be so, as the hydroximolactam **13** (pK_a 4.8–5.2) inhibits both α- and β-glycosidases with similar potency (Figure 20c).[151] Such analogues mark the continuity between neutral lactone-type inhibitors (weak hydrogen-bond acceptors) and strongly basic, fully protonated inhibitors. The K_i values of strongly basic inhibitors such as the amidine **11** and amidinium **12** reflect (partial?) desolvation upon binding to the enzyme, and presumably the absence of a salt bridge to the catalytic acid. The ideal inhibitor will thus be neutral in solution, and well protonated by the enzyme.

The well-established effect of directionality in the strength of salt bridges[152] may play a role in the superior inhibition of α- over β-glucosidases by deoxynojirimycin **4**[39, 153] (Table 11). The ring nitrogen atom of protonated **4** is well positioned to form a hydrogen-bonded ion pair with the (anionic) catalytic nucleophile of α-, but not of β-glucosidases (Figure 21a, b). The reverse is true for isofagomine (**56**),[154–156] in which the position of the (protonated) nitrogen atom is better suited to interact with the catalytic nucleophile of a β-glucosidase

Table 11. IC_{50} values [μM] of deoxynojirimycin (**4**), isofagomine (**56**), azaisofagomine (**57**), deoxygalactostatin (**58**), and *galacto*-isofagomine (**59**).

Enzyme (source)	**4**	**56**	**57**	**58**	**59**
α-glucosidase (brewers' yeast)	12.6	86	3.9		> 2000
β-glucosidase (almonds)	47	0.1	0.65		0.19
α-galactosidase (*E. coli*)	–	–	–	0.0016	200
β-galactosidase (*E. coli*)	–	–	–	0.16	0.012

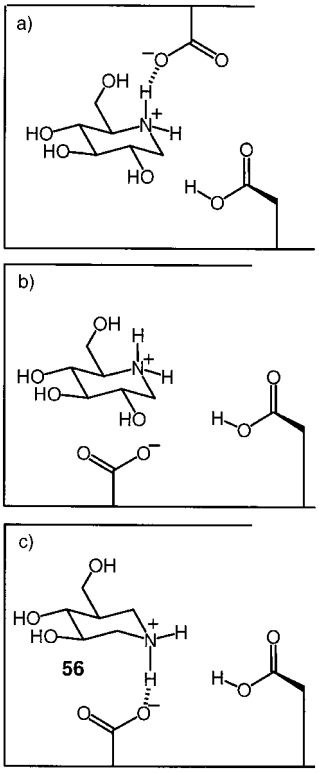

Figure 21. Proposed favored binding interaction of deoxynojirimycin in a α-glucosidase (a), but not in a β-glucosidase (b). c) Favored binding interaction of isofagomine in β-glucosidase.

(Figure 21c), as reflected in its inhibition constants (Table 11). This is consistent with recently results of Bols et al.,[157] who have shown that the analogous piperazine **57**, with a nitrogen

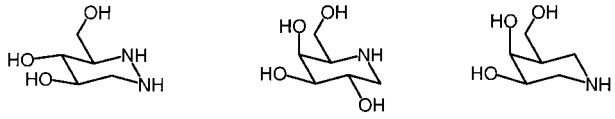

atom in both positions, is less α-selective than deoxynojirimycin (it binds both α- and β-glycosidases more strongly), and less β-selective than isofagomine (it binds α-glycosidases more strongly and β-glycosidases less strongly). The analogous relationship between the position of the ammonium center and the inhibition of α- and β-galactosidases is observed for deoxygalactostatin (**58**)[158] and *galacto*-isofagomine (**59**).[156, 159] Conceivably, calystegin B2[160, 161] can imitate either nojirimycin or isofagomine, depending on the orientation in which it is bound to a glycosidase.

3.5.3.2 Glucosidase or Galactosidase?

The models of the active site of family 1 and 2 glycosidases with bound inhibitors, confirmed by X-ray analyses, also allow a second type of selectivity, or lack of it, to be rationalized. For many years it has been observed that certain β-glucosidases and β-galactosidases only hydrolyze "correctly" configured substrates,[162–167] whereas others show only a minor preference for a specific configuration at C4.[65, 119, 167–171] Much work has been invested in purifying these enzymes to examine

whether these apparently unselective glycosidases are mixtures, but often these enzymes remained poorly selective in spite of their homogeneity.[64, 65] Kinetic results obtained over several decades correlate with the aforementioned classification of glycosidases into families.[52] Thus, β-glucosidases,[116] 6-phospho-β-glucosidases and -galactosidases,[169] and myrosinases (thioglycosidases),[170] all with low *gluco*/*galacto* selectivity, belong to family 1. Glucosidases showing high *gluco* selectivity belong to family 3.[162, 165] Family 2 contains two subfamilies: β-galactosidases, which are strongly *galacto*-selective,[166] and β-glucuronidases, which show low selectivity.[171]

Homology in amino acid sequences implies structural similarity, and indeed much of the active site in the enzymes of families 1 and 2 is similar. The residues responsible for catalysis (both Glu), hydrogen-bonding interactions with HO-C2 and HO-C3 (Asn and His), and hydrophobic interaction with the α face of the substrate (Trp) are observed in all crystal structures,[56, 105, 111, 119] and conserved in all sequences[172] (see Figures 15–17).

Family 1 enzymes have conserved Trp and Gln residues in positions where they can interact with either an axial or an equatorial C4 hydroxyl group (see Figure 22).[173, 174]

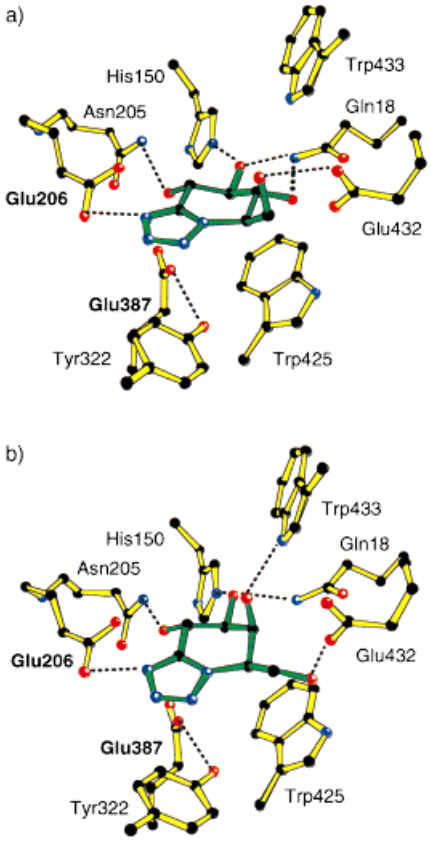

Figure 22. Modeled complexes a) between *S. solfataricus* β-glycosidase (family 1) and *gluco*-tetrazole **20** and b) between *S. solfataricus* β-glycosidase (family 1) and *galacto*-tetrazole **22**.

Both subfamilies of family 2 possess a conserved Asp residue in a position to form a hydrogen bond with an axial C4 hydroxyl group for the representative structures of the *E. coli* β-galactosidase[104] and human β-glucuronidase,[120] which both hydrolyze *galacto*-substrates. These structures are distinguished by the positioning of the conserved Trp residue onto which the pyranose ring stacks. In the human β-glucuronidase, the equatorial C4 hydroxyl group can form a hydrogen bond with the indole nitrogen atom of Trp587 (Figure 23), whereas the equivalent Trp568 in the *E. coli* β-galactosidase (see Figure 15) is shifted upwards, interacts with the hydrophobic face of a galactopyranoside, blocks access to an equatorial hydroxy group, and prevents glucosides from fully entering the active site.

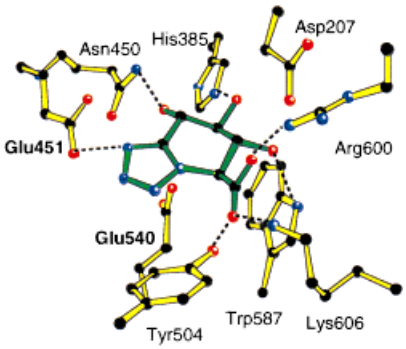

Figure 23. Complex between human β-glucuronidase (family 2) and *gluco*-tetrazole **20**.

So far, no crystal structure has been solved for a family 3 glucosidase, precluding an understanding of the interactions responsible for the high *gluco* selectivity of these enzymes.

4. Aglycon Selectivity—Inhibition by Disaccharide Analogues

Most of the inhibitors discussed in the preceding sections are analogues of the glycon part of the substrate or the transition state. The inclusion of the aglycon part of the natural substrate to the inhibitory glycon portion, for example by the construction of a disaccharide analogue, should ideally lead to increased inhibitory potency and α/β selectivity. A number of research groups have prepared disaccharide analogues of potent inhibitors such as trehazolin,[175] isofagomine,[155] valienamine,[176] 1-deoxynojirimycin,[177–180] 1-deoxymannojirimycin,[181, 182] and other azasugars.[173–190]

The oxime functionality of a hydroximolactam or hydroximolactone is oriented more closely towards the position occupied by the aglycon of a β-glycoside than that of an α-glycoside. A oxime substituent should therefore mimic the aglycon of a β-glycoside more closely than that of an α-glycoside, and a thus substituted hydroximo compound should be a more selective inhibitor of β-glycosidases. The cellobioside analogues **62** and **64** were synthesised by alkylation of the benzyl-protected D-gluconohydroximo-1,5-lactam **19** with the *galacto*-configured triflate **60**, or by condensation of the benzyl-protected thiolactam **18** with the *gluco*-configured hydroxylamines **61** or **63**, followed by debenzylation with lithium in $EtNH_2$. The lactoside analogue **66** was obtained from the protected D-galactonothiolactam **65**.[191]

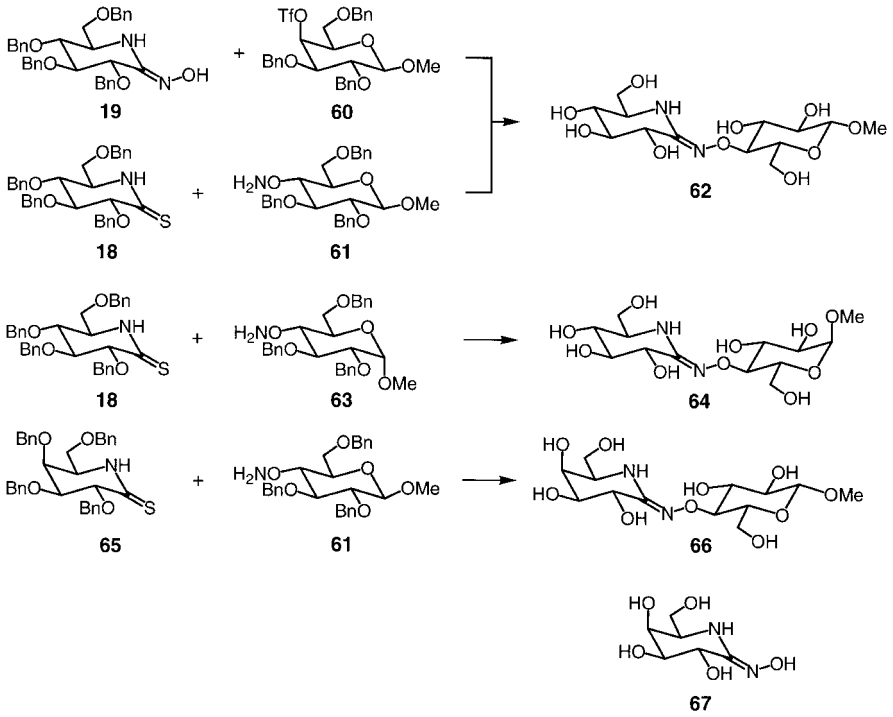

The cellobioside analogues **62** and **64** both inhibit the β-glucosidase from *C. saccharolyticum* as strongly as the unsubstituted hydroximolactam **13**; the second pyranoside ring neither impedes nor enhances the binding to this enzyme (Table 12). However, binding to the yeast α-glucosidase is weakened by a factor of at least 1000, showing that the second pyranoside ring cannot be accommodated in the active site of this glycosidase. The sweet-almond β-glucosidases, with a known preference for a hydrophobic aglycon,[59] are an interesting case: the inhibition by the β-cellobioside analogue **62** is only four times weaker than that by **13**, whereas that by the α-cellobioside **64** is 100 times weaker. This is in keeping with the interaction with (presumably) a hydrophobic and flat aglycon, incompatible with the axial methoxy group of **64**.

The α/β selectivity for the cellobioside analogues **62** and **64** is mirrored by the lactoside analogue **66**. Thus, the potent inhibition of coffee-bean α-galactosidase by the unsubstituted hydroximolactam **67** ($K_i = 5$ μM) is significantly weakened by the introduction of the glucosyl moiety in **66** ($K_i = 250$ μM), whereas both oximolactams **66** and **67** are potent competitive inhibitors of the *E. coli* β-galactosidase (family 2) with a K_i of 100 nM.

The K_i values of **66** (3.3 μM) and **67** (2.5 μM) against the β-glucosidase from *C. saccharolyticum* (family 1) are similar to those for the *gluco*-analogues **13** and **62**, confirming that family 1 glucosidases are not selective for the configuration at C4, and also that the aglycon binding site is adapted for hydrophilic as well as hydrophobic residues. This is in keeping with the role of this enzyme as an *exo*-cellulase, and the observation that it also readily hydrolyzes *p*-nitrophenyl glycosides.[192] For these interpretations, one should not forget that the distance between glycon and aglycon is larger for the oxime ethers than for the disaccharides. Although the glycosidic bond is progressively stretched during cleavage, it is by no means clear how this aspect affects the inhibition by the disaccharide analogues.

The bovine-liver β-galactosidase is inhibited about 100 times more strongly by **67** ($K_i = 10$ μM) than by **66** ($IC_{50} \approx 2.5$ mM), in keeping with the strong preference of the bovine-liver glycosidase for aryl pyranosides. This contrasts somewhat with the results for the inhibition of the sweet-almond β-glucosidases, which also have a preference for aryl pyranoside substrates,[59] but for which the cellobioside analogue **62** binds only four times more weakly than the unsubstituted **13**. It would seem that the aromatic aglycon binding site in the bovine-liver β-glycosidase is more selective than that in the sweet-almond β-glucosidases. Unfortunately the amino acid sequence of neither glycosidase has been reported, which makes it impossible to draw any specific conclusions from these results regarding the structure of their active site, and thus the reasons behind their differing preferences for aromatic aglycons.

5. Concluding Remarks

The synthesis of suitable glycosidase inhibitors, kinetic data, structural information about glycosidases or glycosidase–inhibitor complexes, and the interpretation of these results in the light of the reactivity of organic compounds are ideal prerequisites to elucidate details of enzymic reaction mechanisms. Exact information about these mechanisms, in its turn, allows the rational design of stronger and more selective inhibitors. The consideration of the protonation in

Table 12. K_i and IC_{50} values of the lactam oximes **13**, **62**, **63**, **66**, and **67**.

Enzyme	K_M[a]	pH	K_i [μM] or in italics IC_{50} values [μM]				
			13	**62**	**63**	**66**	**67**
β-glucosidases (almonds)	3.0 (1.2)	6.8	16	*60*	*1000*	–	–
β-glucosidase (*C. saccharolyticum*)	1.2 (1.2)	6.8	3.3	*3.6*	*2.0*	3.3	2.5
α-glucosidase (brewers' yeast)	1.2 (1.2)	6.8	2.9	*2500*	*> 5000*		
β-galactosidase (bovine liver)	0.24 (0.24)	7.0	–	–	–	*2500*	10[58]
β-galactosidase (*E. coli*)	0.04	6.8	–	–	–	0.1	0.1
α-galactosidase (coffee beans)	0.19	6.0	–	–	–	250	5

[a] K_M values [mM] for corresponding 4-nitrophenyl hexopyranosides. In parenthesis, starting concentration of the substrate [mM].

the ring plane, of the direction from which the protonation occurs (*syn* versus *anti* protonators), and of the conformational changes during glycoside cleavage will prove valid in the design of inhibitors. It should be mentioned in this context that recent results from K. Piens in the laboratory of M. Claeyssens (University of Gent) have shown that inhibitors of the hydroximolactam- and imidazole-type inhibit cellobiohydrolyase II (CBH II) of *Trichoderma reesei*, but not cellobiohydrolase I (CBH I). This is consistent with the assignment of CBH I as a *syn* protonator, and suggests that CBH II may be an *anti* protonator. The question of whether similar selectivities exist for the still poorly known glycosyl transferases promises further thrilling studies in the interplay of organic chemistry, enzymology, protein crystallography, and biotechnology.

Particular thanks go to present and past co-workers of the group, to Gideon Davies, Doug Juers, Günter Legler, Michael Sinnott, and Steve Withers for many stimulating discussions, and to Bruno Bernet for his critical help in completing the manuscript. We thank the Swiss National Science Foundation, the Federal Office of Education and Science (BBW 96.0375, EU research program BIO4-CT96-0580), Hoffmann La Roche, and Oxford GlycoSciences for their longstanding financial help.

Received: July 27, 1998 [A 292 IE]
German version: *Angew. Chem.* **1999**, *111*, 794 – 815

[1] G. J. Davies, M. L. Sinnott, S. G. Withers in *Comprehensive Biological Catalysis* (Ed.: M. L. Sinnott), Academic Press, London, **1998**, pp. 119 – 207.
[2] a) *Carbohydrate Mimics* (Ed.: Y. Chapleur), WILEY-VCH, Weinheim, **1998**; b) G. Legler in ref. [2a], pp. 463 – 490.
[3] S. Ogawa in ref. [2a], pp. 87 – 106.
[4] B. Ganem in ref. [2a], pp. 239 – 258.
[5] K. Tatsuta in ref. [2a], pp. 283 – 306.
[6] J.-C. Depezay in ref. [2a], pp. 307 – 326.
[7] M. Bols, *Acc. Chem. Res.* **1998**, *31*, 1 – 8.
[8] J. M. Williams in *Glycopeptides and Related Compounds* (Eds.: D. G. Large, C. D. Warren), Marcel Dekker, New York, **1997**, pp. 505 – 539.
[9] A. White, D. Rose, *Curr. Opin. Struct. Biol.* **1997**, *7*, 645 – 651.
[10] A. De Raadt, C. W. Ekart, M. Ebner, A. E. Stütz, *Top. Curr. Chem.* **1997**, *187*, 157 – 186.
[11] S. Picasso, *Chimia* **1996**, *50*, 648 – 649.
[12] "Identification of the Active Site Residues in Glycosidases": S. G. Withers, *ACS Symp. Ser.* **1996**, *619*, 365 – 380.
[13] G. Davies, B. Henrissat, *Structure* **1995**, *3*, 853 – 859.
[14] S. G. Withers, *Progr. Biotechnol.* **1995**, *10*, 97 – 111.
[15] S. G. Withers, *Pure Appl. Chem.* **1995**, *67*, 1673 – 1682.
[16] G. S. Jacob, *Curr. Opin. Struct. Biol.* **1995**, *5*, 605 – 611.
[17] J. D. McCarter, S. G. Withers, *Curr. Opin. Struct. Biol.* **1994**, *4*, 885 – 892.
[18] V. Jäger, R. Müller, T. Leibold, M. Hein, M. Schwarz, M. Fengler, L. Jaroskova, M. Pätzel, P.-Y. LeRoy, *Bull. Soc. Chim. Belg.* **1994**, *103*, 491 – 507.
[19] G. Legler, *Naturwissenschaften* **1993**, *80*, 397 – 409.
[20] B. Winchester, G. W. J. Fleet, *Glycobiology* **1992**, *2*, 199 – 210.
[21] R. W. Franck, *Bioorg. Chem.* **1991**, *20*, 77 – 88.
[22] A. D. Elbein, *FASEB J.* **1991**, *5*, 3055 – 3063.
[23] D. E. Koshland, *Biol. Rev.* **1953**, *28*, 416 – 436.
[24] C. A. Vernon, *Proc. R. Soc. London B* **1967**, *167*, 389 – 401.
[25] D. C. Phillips, *Proc. Natl. Acad. Sci. USA* **1967**, *57*, 484 – 497.
[26] S. G. Withers, R. A. J. Warren, I. P. Street, K. Rupitz, J. B. Kempton, R. Aebersold, *J. Am. Chem. Soc.* **1990**, *112*, 5887 – 5889.
[27] S. G. Withers, R. Aebersold, *Protein Sci.* **1995**, *4*, 361 – 372.
[28] W. P. Jencks, *Catalysis in Chemistry and Enzymology*, McGraw-Hill, New York, **1969**.
[29] S. V. Evans, L. E. Fellows, E. A. Bell, *Phytochemistry* **1983**, *22*, 768 – 770.
[30] M. P. Dale, H. E. Ensley, K. Kern, K. A. R. Sastry, L. D. Byers, *Biochemistry* **1985**, *24*, 3530 – 3539.
[31] P. A. Fowler, A. H. Haines, R. J. K. Taylor, E. J. T. Chrystal, M. B. Gravestock, *Carbohydr. Res.* **1993**, *246*, 377 – 381.
[32] G. Legler, A. Korth, A. Berger, C. Ekhart, G. Gradnig, A. E. Stütz, *Carbohydr. Res.* **1993**, *250*, 67 – 77.
[33] S. Ezaki, *J. Biochem. (Tokyo)* **1940**, *32*, 91 – 105.
[34] K. Horikoshi, *J. Biochem. (Tokyo)* **1942**, *35*, 39 – 46.
[35] G. A. Levvy, *J. Biochem. (Tokyo)* **1952**, *52*, 464 – 472.
[36] J. Conchie, G. A. Levvy, *Biochem. J.* **1957**, *65*, 389 – 395.
[37] G. A. Levvy, S. M. Snaith, *Adv. Enzymol. Relat. Areas Mol. Biol.* **1972**, *36*, 151 – 181.
[38] D. H. Leaback, *Biochem. Biophys. Res. Commun.* **1968**, *32*, 1025 – 1030.
[39] E. T. Reese, F. W. Parrish, M. Ettlinger, *Carbohydr. Res.* **1971**, *18*, 381 – 388.
[40] For space-filling properties or "steric complementariness", see ref. [41].
[41] L. Pauling, *Chem. Eng. News* **1946**, *24*, 1375 – 1377.
[42] R. Wolfenden, *Acc. Chem. Res.* **1972**, *5*, 10 – 18.
[43] T. Kajimoto, K. K.-C. Liu, R. L. Pederson, Z. Zhong, Y. Ichikawa, J. A. Porco, C.-H. Wong, *J. Am. Chem. Soc.* **1991**, *113*, 6187 – 6196.
[44] B. Ganem, G. Papandreou, *J. Am. Chem. Soc.* **1991**, *113*, 8984 – 8985.
[45] A. Vasella, P. Ermert, R. Hoos, A. B. Naughton, K. Rupitz, W. Thiel, M. Weber, W. Weber, S. G. Withers in *Complex Carbohydrates in Drug Research* (Eds.: K. Bock, H. Clausen), Munksgaard, Kopenhagen, **1994**, pp. 134 – 150 (*Alfred Benzon Symposium 36*).
[46] L. N. Johnson, D. C. Phillips, *Nature* **1965**, *206*, 761 – 763.
[47] I. I. Secemski, S. S. Lehrer, G. E. Lienhard, *J. Biol. Chem.* **1972**, *247*, 4740 – 4748.
[48] L. O. Ford, L. N. Johnson, P. A. Machin, D. C. Phillips, R. Tjian, *J. Mol. Biol.* **1974**, *88*, 349 – 371.
[49] A. Warshel, *Proc. Natl. Acad. Sci. USA* **1978**, *75*, 5250 – 5254.
[50] A. Warshel, *Acc. Chem. Res.* **1981**, *14*, 284 – 290.
[51] B. Henrissat, *Biochem. J.* **1991**, *280*, 309 – 316.
[52] B. Henrissat, G. Davies, *Curr. Opin. Struct. Biol.* **1997**, *7*, 637 – 644.
[53] P. Lalégerie, G. Legler, J. M. Yon, *Biochimie* **1982**, *64*, 977 – 1000.
[54] R. Saul, R. J. Molyneux, A. D. Elbein, *Arch. Biochem. Biophys.* **1984**, *230*, 668 – 675.
[55] T. E. Couling, R. Goodey, *Biochem. J.* **1970**, *119*, 303 – 306.
[56] The X-ray structure of a complex between a β-glucosidase and the ring-opened form of gluconolactone has been solved recently: J. Sanz-Aparicio, J. A. Hermoso, M. Martínez-Ripoll, J. L. Lequerica, J. Polaina, *J. Mol. Biol.* **1998**, *275*, 491 – 502.
[57] D. Beer, A. Vasella, *Helv. Chim. Acta* **1986**, *69*, 267 – 270.
[58] G. Papandreou, M. K. Tong, B. Ganem, *J. Am. Chem. Soc.* **1993**, *115*, 11 682 – 11 690.
[59] W. Hösel, E. E. Conn, *Trends Biochem. Sci.* **1982**, *1*, 219 – 221.
[60] M. K. Tong, G. Papandreou, B. Ganem, *J. Am. Chem. Soc.* **1990**, *112*, 6137 – 6139.
[61] G. Legler, M.-T. Finken, S. Felsch, *Carbohydr. Res.* **1996**, *292*, 91 – 101.
[62] R. Hoos, A. B. Naughton, A. Vasella, *Helv. Chim. Acta* **1993**, *76*, 1802 – 1807.
[63] R. Hoos, A. B. Naughton, W. Thiel, A. Vasella, W. Weber, K. Rupitz, S. G. Withers, *Helv. Chim. Acta* **1993**, *76*, 2666 – 2686.
[64] A. K. Grover, D. D. MacMurchie, R. J. Cushley, *Biochim. Biophys. Acta* **1977**, *482*, 98 – 108.
[65] J. J. Distler, G. W. Jourdian, *Arch. Biochem. Biophys.* **1977**, *178*, 631 – 643.
[66] P. Ermert, A. Vasella, *Helv. Chim. Acta* **1991**, *74*, 2043 – 2053.
[67] P. Ermert, A. Vasella, M. Weber, K. Rupitz, S. G. Withers, *Carbohydr. Res.* **1993**, *250*, 113 – 125.
[68] T. D. Heightman, P. Ermert, D. Klein, A. Vasella, *Helv. Chim. Acta* **1995**, *78*, 514 – 532.
[69] S. Vonhoff, A. Vasella, *Synth. Commun.*, in press.

[70] H. Therisod, Y. Letourneux, M. Therisod, *Bioorg. Med. Chem. Lett.* **1998**, *8*, 371 – 372.
[71] S. G. Withers, K. Rupitz, D. Trimbur, R. A. J. Warren, *Biochemistry* **1992**, *31*, 9979 – 9985.
[72] Y.-K. Li, L. D. Byers, *Biochim. Biophys. Acta* **1989**, *999*, 227 – 232.
[73] R. A. Field, A. H. Haines, E. J. T. Chrystal, M. C. Luszniak, *Biochem. J.* **1991**, *274*, 885 – 889.
[74] T. Granier, A. Vasella, *Helv. Chim. Acta* **1995**, *78*, 1738 – 1746.
[75] G. Legler, E. Bieberich, *Arch. Biochem. Biophys.* **1988**, *260*, 437 – 442.
[76] G. Legler, *Adv. Carbohydr. Chem. Biochem.* **1990**, *48*, 333 – 335.
[77] T. Aoyagi, H. Suda, K. Uotani, F. Kojima, T. Aoyama, K. Horiguchi, M. Hamada, T. Takeuchi, *J. Antibiot.* **1992**, *45*, 1404 – 1408.
[78] T. Aoyama, H. Naganawa, H. Suda, K. Uotani, T. Aoyagi, T. Takeuchi, *J. Antibiot.* **1992**, *45*, 1557 – 1558.
[79] K. Tatsuta, S. Miura, S. Ohta, H. Gunji, *J. Antibiot.* **1995**, *48*, 286 – 288.
[80] K. Tatsuta, S. Miura, S. Ohta, H. Gunji, *Tetrahedron Lett.* **1995**, *36*, 1085 – 1088.
[81] K. Tatsuta, S. Miura, *Tetrahedron Lett.* **1995**, *36*, 6721 – 6724.
[82] K. Tatsuta, S. Miura, H. Gunji, *Bull. Chem. Soc. Jpn.* **1997**, *70*, 427 – 436.
[83] M. Langer, A. Pauling, J. Rétey, *Angew. Chem.* **1995**, *107*, 1585 – 1587; *Angew. Chem. Int. Ed. Engl.* **1995**, *34*, 1464 – 1465.
[84] J. Winter, J. Rétey, *Chem. Eur. J.* **1997**, *3*, 410 – 416.
[85] T. Granier, F. Gaiser, L. Hintermann, A. Vasella, *Helv. Chim. Acta* **1997**, *80*, 1443 – 1456.
[86] N. Panday, T. Granier, A. Vasella, *Helv. Chim. Acta* **1998**, *81*, 475 – 490.
[87] D. C. Phillips, *Sci. Am.* **1966**, *215*(5), 78 – 90.
[88] A. J. Kirby, *Nat. Struct. Biol.* **1996**, *3*, 107 – 108.
[89] H. Thøgersen, R. U. Lemieux, K. Bock, B. Meyer, *Can. J. Chem.* **1982**, *60*, 44 – 57.
[90] The objection that this would specifically curtail the *exo* anomeric interaction between this lone pair and the endocyclic C–O bond is not valid: protonation of the other lone pair would raise the formal electronegativity of the oxygen and thus equally impair the *exo* anomeric interaction.
[91] L. P. McIntosh, G. Hand, P. E. Johnson, M. D. Joshi, M. Körner, L. A. Plesniak, L. Ziser, W. W. Wakarchuk, S. G. Withers, *Biochemistry* **1996**, *35*, 9958 – 9966.
[92] T. D. Heightman, M. Locatelli, A. Vasella, *Helv. Chim. Acta* **1996**, *79*, 2190 – 2200.
[93] M. J. Kamlet, J. L. M. Abboud, R. W. Taft, *Progr. Phys. Org. Chem.* **1981**, *13*, 485 – 630.
[94] M. D. Joesten, *J. Chem. Educ.* **1982**, *59*, 362 – 366.
[95] E. P. Mitchell, S. G. Withers, P. Ermert, A. T. Vasella, E. F. Garman, N. G. Oikonomakos, L. N. Johnson, *Biochemistry* **1996**, *35*, 7341 – 7355.
[96] P. J. McLaughlin, D. I. Stuart, H. W. Klein, N. G. Oikonomakos, L. N. Johnson, *Biochemistry* **1984**, *23*, 5862 – 5873.
[97] H. W. Klein, M. J. Im, D. Palm, *Eur. J. Biochem.* **1986**, *157*, 107 – 114.
[98] T. Granier, N. Panday, A. Vasella, *Helv. Chim. Acta* **1997**, *80*, 979 – 987.
[99] T. D. Heightman, Dissertation, ETH Zürich, **1998**.
[100] K. Tatsuta, Y. Ikeda, S. Miura, *J. Antibiot.* **1996**, *49*, 836 – 838.
[101] T. D. Heightman, A. Vasella, K. E. Tsitsanou, S. E. Zographos, V. T. Skamnaki, N. Oikonomakos, *Helv. Chim. Acta* **1998**, *81*, 853 – 864.
[102] M. N. Namchuk, S. G. Withers, *Biochemistry* **1995**, *34*, 16194 – 16202.
[103] In most cases no inhibition was observed at concentration of 8 mM for the 1,2,3-triazoles **53** and **54**, whereas the K_i values for the tetrazoles **24** and **25** refer to concentrations giving close to 50 % inhibition. The comparison of these values thereby gives a lower limit, and the real difference is probably significantly larger.
[104] R. H. Jacobsen, X.-J. Zhang, R. F. DuBose, B. W. Matthews, *Nature* **1994**, *369*, 761 – 766.
[105] T. Barrett, C. G. Suresh, S. P. Tolley, E. J. Dodson, M. A. Hughes, *Structure* **1995**, *3*, 951 – 960.
[106] C. Wiesmann, G. Beste, W. Hengstenberg, G. E. Schulz, *Structure* **1995**, *3*, 961 – 968.
[107] A. White, D. Tull, K. Johns, S. G. Withers, D. R. Rose, *Nat. Struct. Biol.* **1996**, *3*, 149 – 154.
[108] S. G. Withers, I. P. Street, *J. Am. Chem. Soc.* **1988**, *110*, 8551 – 8553.
[109] F. A. Quiocho, *Pure Appl. Chem.* **1989**, *61*, 1293 – 1306.
[110] J. Sakon, W. S. Adney, M. E. Himmel, S. R. Thomas, P. A. Karplus, *Biochemistry* **1996**, *35*, 10648 – 10660.
[111] C. Wiesmann, W. Hengstenberg, G. E. Schulz, *J. Mol. Biol.* **1997**, *269*, 851 – 860.
[112] W. P. Burmeister, S. Cottaz, H. Driguez, R. Iori, S. Palmieri, B. Henrissat, *Structure* **1997**, *5*, 663 – 675.
[113] R. Dominguez, H. Souchon, M.-B. Lascombe, P. M. Alzari, *J. Mol. Biol.* **1996**, *257*, 1042 – 1051.
[114] M. Qian, R. Haser, F. Payan, *J. Mol. Biol.* **1993**, *231*, 785 – 799.
[115] C. Gilles, J.-P. Astier, G. Marchis-Mouren, C. Cambillau, F. Payan, *Eur. J. Biochem.* **1996**, *238*, 561 – 569.
[116] A. M. Brzozowski, G. Davies, *Biochemistry* **1997**, *36*, 10837 – 10845.
[117] B. Strokopytov, R. M. A. Knegtel, D. Penninga, H. J. Rozeboom, K. H. Kalk, L. Dijkhuizen, B. W. Dijkstra, *Biochemistry* **1996**, *35*, 4241 – 4249.
[118] I. Tews, A. Perrakis, A. Oppenheim, Z. Dauter, K. S. Wilson, C. E. Vorgias, *Nat. Struct. Biol.* **1996**, *3*, 638 – 648.
[119] C. Aguilar, I. Sanderson, M. Moracci, M. Ciaramella, R. Nucci, M. Rossi, L. H. Pearl, *J. Mol. Biol.* **1997**, *271*, 789 – 802.
[120] S. Jain, W. B. Drendel, Z.-W. Chen, F. S. Mathews, W. S. Sly, J. H. Grubb, *Nat. Struct. Biol.* **1996**, *3*, 375 – 381.
[121] R. Dominguez, H. Souchon, M.-B. Lascombe, P. M. Alzari, *Nat. Struct. Biol.* **1995**, *2*, 569 – 576.
[122] G. W. Harris, J. A. Jenkins, I. Connerton, N. Cummings, L. L. Leggio, M. Scott, G. P. Hazlewood, J. I. Laurie, H. J. Gilbert, R. W. Pickersgill, *Structure* **1994**, *2*, 1107 – 1116.
[123] G. Sulzenbacher, H. Driguez, B. Henrissat, M. Schülein, G. J. Davies, *Biochemistry* **1996**, *35*, 15280 – 15287.
[124] D. Irwin, D. H. Shin, S. Zhang, B. K. Barr, J. Sakon, P. A. Karplus, D. B. Wilson, *J. Bacteriol.* **1998**, *180*, 1709 – 1714.
[125] W. W. Wakarchuk, R. L. Campbell, W. L. Sung, J. Davoodi, M. Yaguchi, *Protein Sci.* **1994**, *3*, 467 – 475.
[126] J. A. Kelly, A. R. Sielecki, B. D. Sykes, M. N. G. James, D. C. Phillips, *Nature* **1979**, *282*, 875 – 878.
[127] A. T. Hadfield, D. J. Harvey, D. B. Archer, D. A. MacKenzie, D. J. Jeenes, S. E. Radford, G. Lowe, C. M. Dobson, L. N. Johnson, *J. Mol. Biol.* **1994**, *243*, 856 – 872.
[128] N. C. J. Strynadka, M. N. G. James, *J. Mol. Biol.* **1991**, *220*, 401 – 424.
[129] L. H. Weaver, M. G. Grütter, B. W. Matthews, *J. Mol. Biol.* **1995**, *245*, 54 – 68.
[130] G. Davies, S. P. Tolley, B. Henrissat, C. Hjort, M. Schülein, *Biochemistry* **1995**, *34*, 16210 – 16220.
[131] C. Divne, J. Ståhlberg, T. Reinikainen, L. Ruohonen, G. Pettersson, J. K. C. Knowles, T. T. Teeri, T. A. Jones, *Science* **1994**, *265*, 524 – 528.
[132] G. J. Kleywegt, J.-Y. Zou, C. Divne, G. J. Davies, I. Sinning, J. Ståhlberg, T. Reinikainen, M. Srisodsuk, T. T. Teeri, T. A. Jones, *J. Mol. Biol.* **1997**, *272*, 383 – 397.
[133] M. Juy, A. G. Amit, P. M. Alzari, R. J. Poljak, M. Claeyssens, P. Béguin, J.-P. Aubert, *Nature* **1992**, *357*, 89 – 91.
[134] A. Törrönen, J. Rouvinen, *Biochemistry* **1995**, *34*, 847 – 856.
[135] R. Havukainen, A. Törrönen, T. Laitinen, J. Rouvinen, *Biochemistry* **1996**, *35*, 9617 – 9624.
[136] T. Keitel, O. Simon, R. Borriss, U. Heinemann, *Proc. Natl. Acad. Sci. USA* **1993**, *90*, 5287 – 5291.
[137] M. Hahn, T. Keitel, U. Heinemann, *Eur. J. Biochem.* **1995**, *232*, 849 – 858.
[138] A. Perrakis, I. Tews, Z. Dauter, A. B. Oppenheim, I. Chet, K. S. Wilson, C. E. Vorgias, *Structure* **1994**, *2*, 1169 – 1180.
[139] P. J. Hart, H. D. Pfluger, A. F. Monzingo, T. Hollis, J. D. Robertus, *J. Mol. Biol.* **1995**, *248*, 402 – 413.
[140] J. Rouvinen, T. Bergfors, T. Teeri, J. K. C. Knowles, T. A. Jones, *Science* **1990**, *249*, 380 – 386.
[141] P. M. Alzari, H. Souchon, R. Dominguez, *Structure* **1996**, *4*, 265 – 275.
[142] U. Derewenda, L. Swenson, R. Green, Y. Wei, R. Morosoli, F. Shareck, D. Kluepfel, Z. S. Derewenda, *J. Biol. Chem.* **1994**, *269*, 20811 – 20814.
[143] J. N. Varghese, T. P. J. Garrett, P. M. Colman, L. Chen, P. B. Høj, G. B. Fincher, *Proc. Natl. Acad. Sci. USA* **1994**, *91*, 2785 – 2789.
[144] V. H. Rao, C. D. Guan, P. Vanroey, *Structure* **1995**, *3*, 449 – 457.

[145] J. Sakon, P. Irwin, D. B. Wilson, P. A. Karplus, *Nat. Struct. Biol.* **1997**, *4*, 810 – 818.
[146] P. Deslongchamps, *Stereoelectronic Effects in Organic Chemistry*, Pergamon, Oxford, **1983**.
[147] G. J. Davies, *Biochem. Soc. Trans.* **1998**, *26*, 167 – 173. Coordinates for this structure have not been released (May 1998).
[148] I. Tews, A. C. Terwisscha van Scheltinga, A. Perrakis, K. S. Wilson, B. W. Dijkstra, *J. Am. Chem. Soc.* **1997**, *119*, 7954 – 7959.
[149] D. Beer, Dissertation, Universität Zürich, **1989**.
[150] A. E. Aleshin, B. Stoffer, L. M. Firsov, B. Svensson, R. B. Honzatko, *Biochemistry* **1996**, *35*, 8319 – 8328.
[151] R. Hoos, A. Vasella, K. Rupitz, S. G. Withers, *Carbohydr. Res.* **1997**, *298*, 291 – 298.
[152] G. A. Jeffrey, W. Saenger, *Hydrogen Bonding in Biological Structures*, Springer, Berlin, **1991**.
[153] T. Niwa, S. Inouye, T. Tsuruoka, Y. Koaze, T. Niida, *Agr. Biol. Chem.* **1970**, *34*, 966 – 968.
[154] T. M. Jespersen, W. Dong, M. R. Seirks, T. Skrydstrup, I. Lundt, M. Bols, *Angew. Chem.* **1994**, *106*, 1858 – 1860; *Angew. Chem. Int. Ed. Engl.* **1994**, *33*, 1778 – 1779.
[155] W. Dong, T. Jespersen, M. Bols, T. Skrydstrup, M. Sierks, *Biochemistry* **1996**, *35*, 2788 – 2795.
[156] Y. Ichikawa, Y. Igarashi, M. Ichikawa, Y. Suhara, *J. Am. Chem. Soc.* **1998**, *120*, 3007 – 3018.
[157] M. Bols, R. G. Hazell, I. B. Thomsen, *Chem. Eur. J.* **1997**, *3*, 940 – 947.
[158] G. Legler, S. Pohl, *Carbohydr. Res.* **1986**, *155*, 119 – 129.
[159] Y. Ichikawa, Y. Igarashi, *Tetrahedron Lett.* **1995**, *36*, 4585 – 4586.
[160] R. J. Molyneux, Y. T. Pan, A. Goldmann, D. A. Tepfer, A. D. Elbein, *Arch. Biochem. Biophys.* **1993**, *301*, 81 – 88.
[161] N. Asano, A. Kato, H. Kizu, K. Matsui, R. C. Griffiths, M. G. Jones, A. A. Watson, R. J. Nash, *Carbohydr. Res.* **1997**, *304*, 173 – 178.
[162] F. Gräbnitz, M. Seiss, K. P. Rücknagel, W. L. Staudenbauer, *Eur. J. Biochem.* **1991**, *200*, 301 – 309.
[163] G. Youatt, *Aust. J. Biol. Sci.* **1958**, *11*, 209 – 217.
[164] F. Gräbnitz, W. L. Staudenbauer, *Biotechnol. Lett.* **1988**, *10*, 73 – 78.
[165] I. A. Kataeva, N. A. Chuvil'skaya, N. P. Golovchenko, V. K. Akimenko, *Biokhimiya (Moscow)* **1991**, *56*, 1429 – 1438.
[166] J. Monod, G. Cohen-Bazire, M. Cohn, *Biochem. Biophys. Acta* **1951**, *7*, 585 – 599.
[167] S. Veibel in *The Enzymes, The Chemistry and Mechanism of Action, Vol. 1, Part 1* (Eds.: J. B. Sumner, K. Myrbäck), Academic Press, New York, **1951**, pp. 583 – 620.
[168] H. Skovbjerg, H. Sjöström, O. Norén, *Eur. J. Biochem.* **1981**, *114*, 653 – 661.
[169] E. Witt, R. Frank, W. Hengstenberg, *Protein Eng.* **1993**, *6*, 913 – 920.
[170] I. Goodman, J. R. Fouts, E. Bresnick, R. Menegas, G. H. Hitchings, *Science* **1959**, *130*, 450 – 451.
[171] C. A. Marsh, G. A. Levvy, *Biochem. J.* **1958**, *68*, 610 – 617.
[172] Sequences are available on the Internet from SWISSPROT http://www.expasy.ch/sprot/
[173] While this manuscript was in preparation, Sanz-Aparicio et al. assigned the same roles to the conserved Trp and Gln residues (see ref. [56]).
[174] In the *Sinapis alpis* myrosinase (family 1) this Trp is replaced by Phe, leaving an empty space occupied by a water molecule in the complex with a *gluco*-configured inhibitor, which may accommodate the hydroxyl group of a *galacto*-configured substrate (see ref. [112]).
[175] S. Knapp, A. Purandare, K. Rupitz, S. G. Withers, *J. Am. Chem. Soc.* **1994**, *116*, 7461 – 7462.
[176] S. Knapp, A. B. J. Naughton, T. G. M. Dhar, *Tetrahedron Lett.* **1992**, *33*, 1025 – 1028.
[177] P. S. Liu, *J. Org. Chem.* **1987**, *52*, 4717 – 4721.
[178] P. B. Anzeveno, L. J. Creemer, J. K. Daniel, C.-H. R. King, P. S. Liu, *J. Org. Chem.* **1989**, *54*, 2539 – 2542.
[179] C. R. Johnson, M. W. Miller, A. Golebiowski, H. Sundram, M. B. Ksebati, *Tetrahedron Lett.* **1994**, *35*, 8991 – 8994.
[180] O. M. Saavedra, O. R. Martin, *J. Org. Chem.* **1996**, *61*, 6987 – 6993.
[181] C. R. Johnson, B. A. Johns, *J. Org. Chem.* **1997**, *62*, 6046 – 6050.
[182] B. A. Johns, Y. T. Pan, A. D. Elbein, C. R. Johnson, *J. Am. Chem. Soc.* **1997**, *119*, 4856 – 4865.
[183] S. Knapp, Y. H. Choe, E. Reilly, *Tetrahedron Lett.* **1993**, *34*, 4443 – 4446.
[184] K. Suzuki, H. Hashimoto, *Tetrahedron Lett.* **1994**, *35*, 4119 – 4122.
[185] J. Lehmann, B. Rob, H.-A. Wagenknecht, *Carbohydr. Res.* **1995**, *278*, 167 – 180.
[186] K. Suzuki, T. Fujii, K. Sato, H. Hashimoto, *Tetrahedron Lett.* **1996**, *37*, 5921 – 5924.
[187] G. Legler, M.-T. Finken, *Carbohydr. Res.* **1996**, *292*, 103 – 115.
[188] A. Baudat, P. Vogel, *J. Org. Chem.* **1997**, *62*, 6252 – 6260.
[189] K. Krähenbühl, S. Picasso, P. Vogel, *Bioorg. Med. Chem. Lett.* **1997**, *7*, 893 – 896.
[190] A. H. Haines, I. Carvalho, *Chem. Commun.* **1998**, 817 – 818.
[191] S. Vonhoff, T. D. Heightman, A. Vasella, *Helv. Chim. Acta* **1998**, *81*, 1710 – 1725.
[192] D. R. Love, R. Fisher, P. L. Bergquist, *Mol. Gen. Genet.* **1988**, *213*, 84 – 92.